



Measurements of the underlying-event properties with the ATLAS detector



Yuri Kulchitsky

Institute of Physics, National Academy of Sciences, Minsk, Belarus

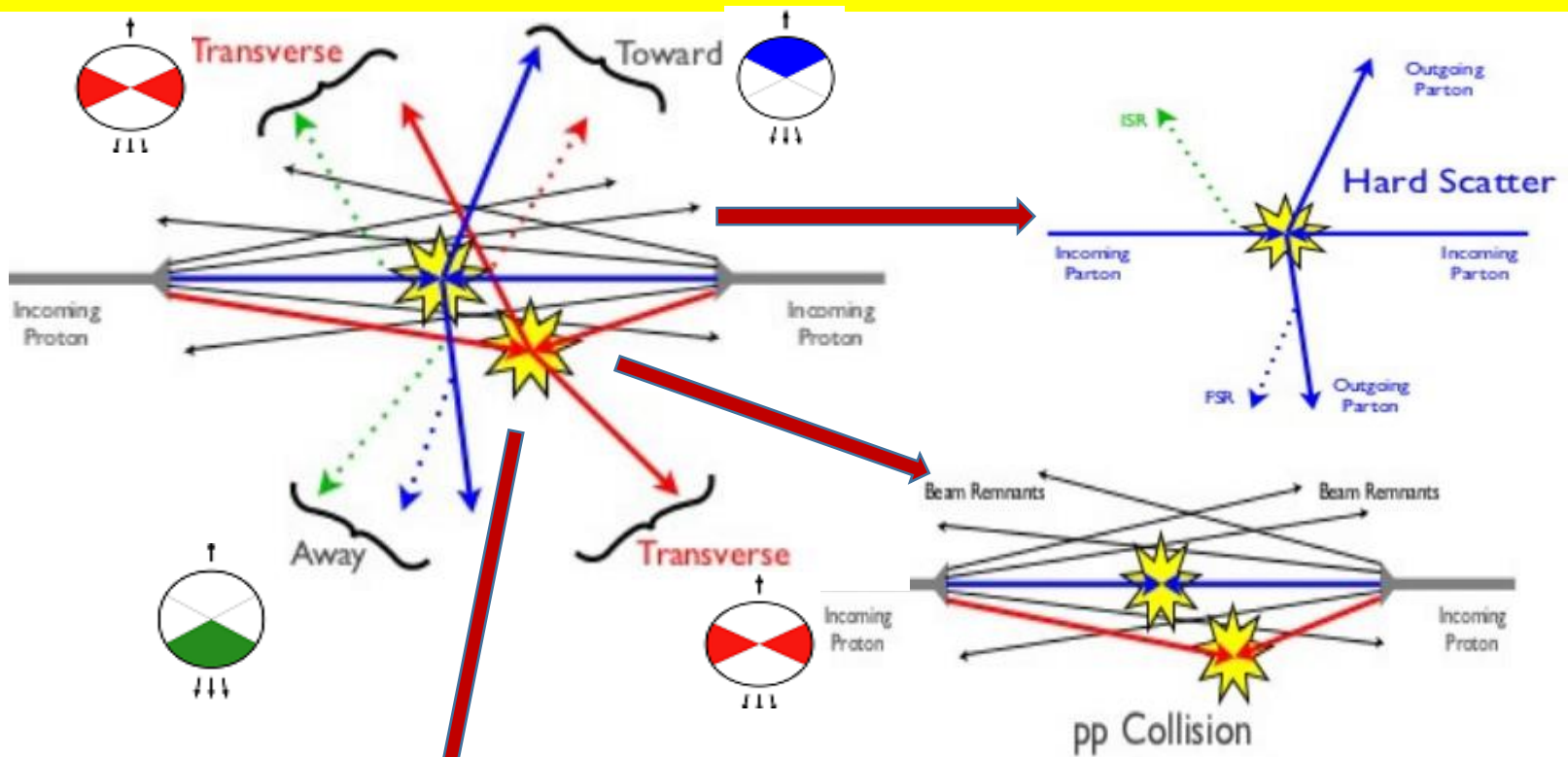
JINR, Dubna, Russia

on behalf of the ATLAS Collaboration



The 24th Low-x Meeting

Károly Róbert College, Gyöngyös, Hungary, 6 – 11 June 2016



The underlying event (UE) is defined as the activity accompanying any hard scattering in a event

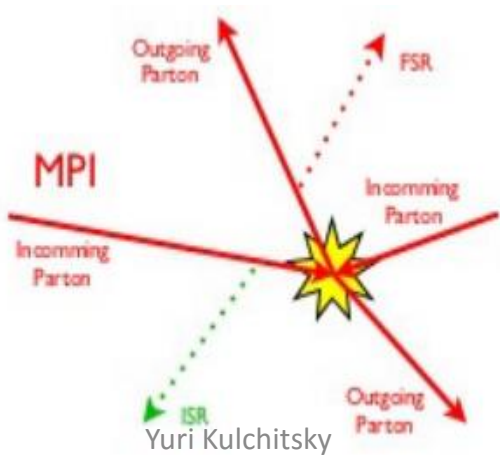
Underling event:

1. Multiple parton interactions (MPI)
2. Initial & Final state gluon radiation (ISR, FSR)
3. Partons not participating in a hard scattering process (beam remnants)

Low-x 2016

Motivation

- Underlying event irreducible background at LHC
- Not understood from first principles in Monte-Carlo models
- Data need for test and constrain model parameters, motivate development
- Analysis are sensitive to multiple parton interactions
- New way of measuring underlying event using event shapes in Drell-Yan events
- First study of the UE at 13 TeV (with leading track)

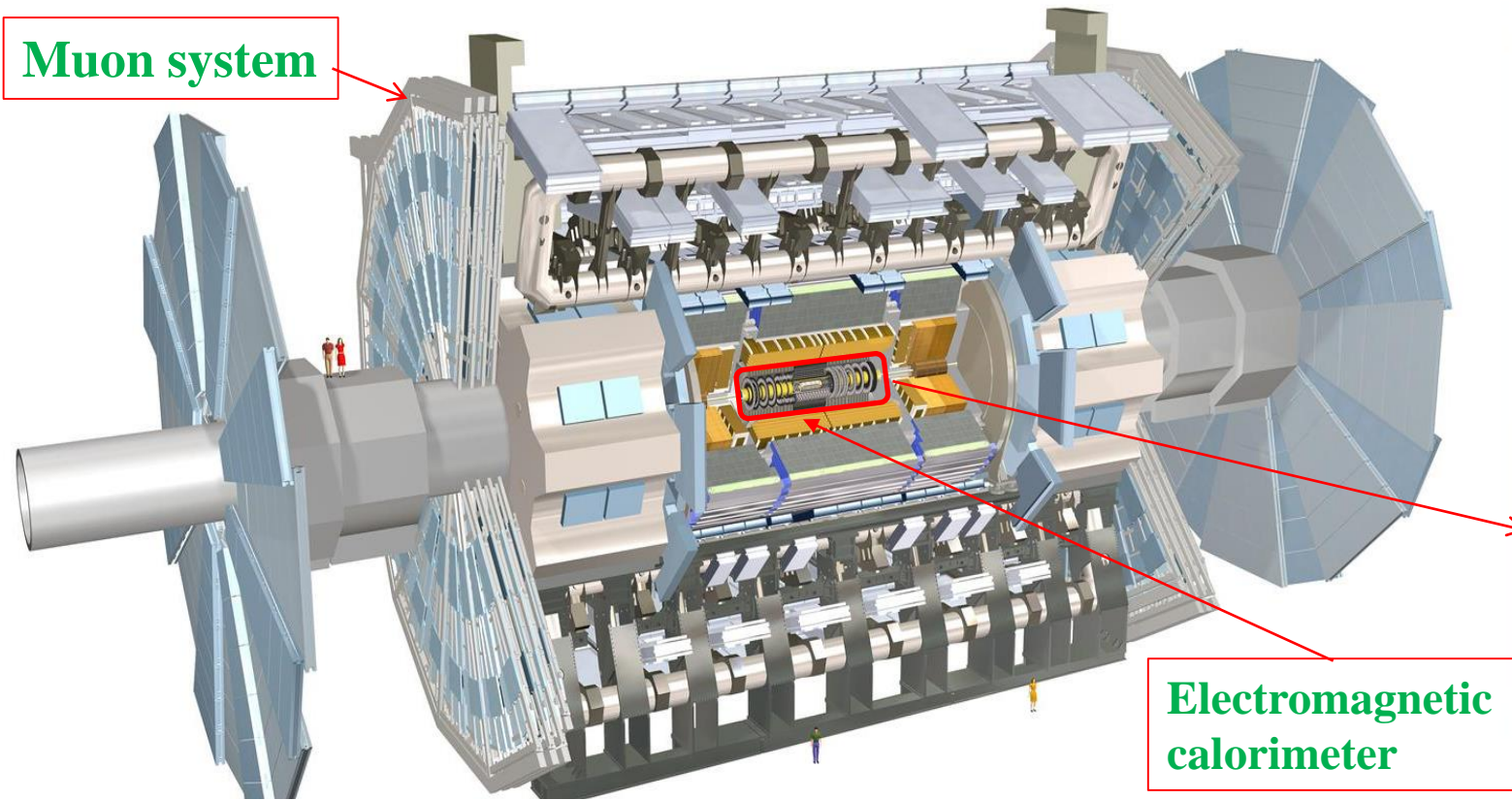


ATLAS detector

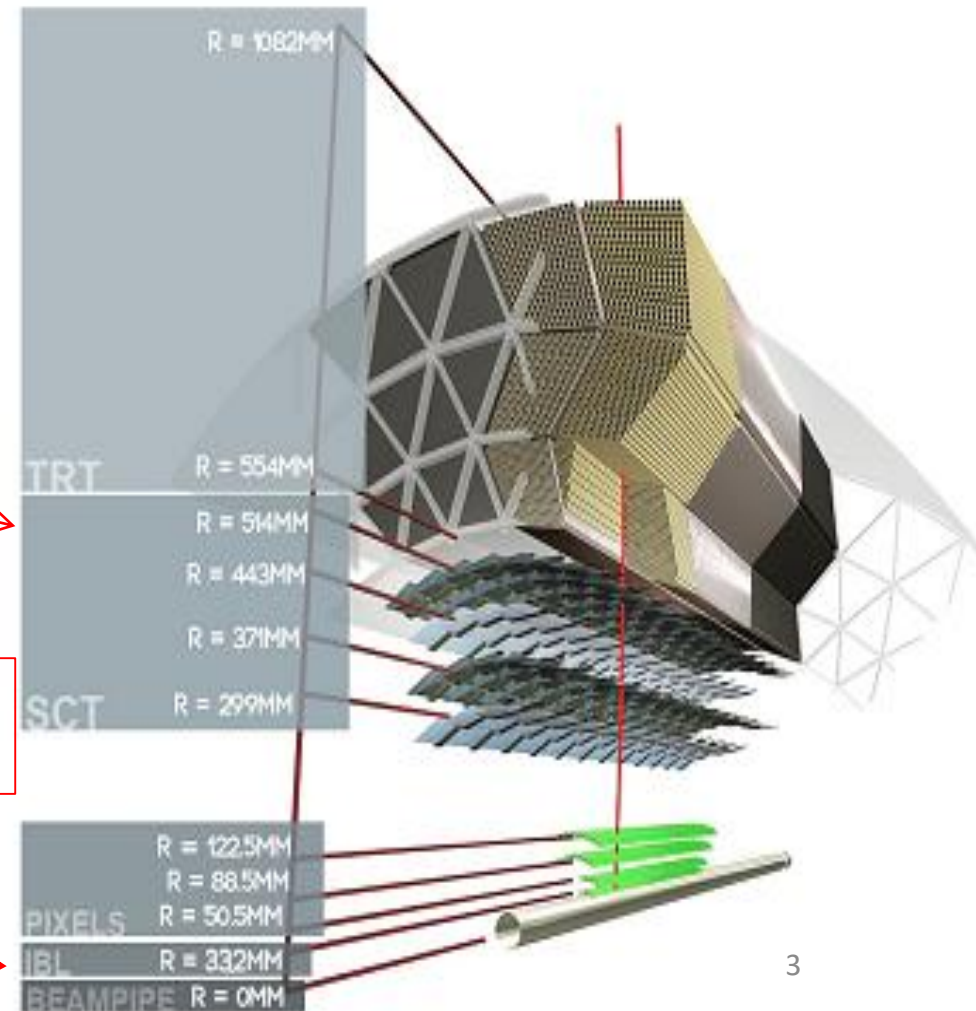
The focus of ATLAS is high- p_T physics, and also provides a window onto important *softer QCD processes*. These have intrinsic interest but also the understanding of underpins searches for new physics.

- ▶ *Underlying event in the event-shape observables in Drell-Yan $Z \rightarrow l^+l^-$ events in pp at 7 TeV* (arXiv:1602.08980)
- ▶ *The leading track underlying event distributions in pp collisions at $\sqrt{s} = 13$ TeV* (ATL-PHYS-PUB-2015-019)

Muon system



Electromagnetic calorimeter



ATLAS Inner Detector (ID) main tracking device: Consists of **Pixel**, **Silicon strip (SCT)** and **drift tube (TRT)** detectors. Single hit resolution between 10 μm (Pixel) and 130 μm (TRT). New in Run2: *Insertable B-Layer (IBL)*

➤ Data

- ❑ About **1.1 fb⁻¹** of data in **pp**-interactions at **7 TeV**
- ❑ **260 k** selected electron channel events, **Z → e⁺e⁻**
- ❑ **410 k** selected muon channel events, **Z → μ⁺μ⁻**

➤ Event selection

❑ Electron cuts:

- $|\eta| < 2.4$, excluding crack region $1.37 < |\eta| < 1.52$
- p_T cluster ≥ 20 GeV
- $|d_0^{PV}| < 5$ mm

❑ Muon cuts:

- $|\eta| < 2.4$
- $p_T \geq 20$ GeV
- $|d_0^{PV}| < 3 \sigma_{d0}$, σ_{d0} is d_0^{PV} resolution
- $|z_0^{PV}| < 10$ mm

❑ Z boson cuts:

- Exactly **two opposite-sign leptons**
- Invariant mass **$66 \text{ GeV} < m_{ll} < 116 \text{ GeV}$**

❑ Primary vertex

- More than 1 track with $p_T > 400$ MeV
- Vertex with highest $\Sigma(p_T^{\text{trk}})^2$

❑ Track selection (similar at 13 TeV; more information in Valentina Cairo MB@ATLAS report)

- ≥ 1 hit in the Pixel subdetector
- ≥ 6 SCT hits;
- $p_T > 500$ MeV and $|\eta| < 2.5$
- $|d_0^{PV}| < 1.5$ mm
- $|z_0^{PV} \sin \theta| < 1.5$ mm
- χ^2 cut for tracks with $p_T^{\text{trk}} > 10$ GeV

➤ Monte Carlo models:

Generator	Version	Tune	PDF	Focus of Tune
Pythia 8	8.212	Monash	NNPDF2.3 LO	MB/UE
Sherpa	2.2.0	Default	NNPDF3.0 NNLO	UE
Herwig 7	7.0	Default	MMHT2014	UE

Distributions $f_O = \frac{1}{N_{ev}} \frac{dN}{dO}$ were measured for all selected events, N_{ev} , with primary charged particles in the region $p_T > 0.5$ GeV and $|\eta| < 2.5$ for the following observables O :

- **The charged-particle multiplicity, N_{ch} .**
- **The scalar sum of transverse momenta** of selected charged particles ($n_{sel} \geq 0$) $\sum p_T$.
- **Beam thrust:** $B = \sum p_T e^{-|\eta|}$. This is similar to $\sum p_T$ but each particle is weighted by a factor $e^{-|\eta|}$. For $n_{sel} \geq 2$. Contributions from particles with large $|\eta|$ are suppressed to one with $\eta \sim 0$.
- **Transverse thrust:** $T = \max_{\vec{n}_T} \frac{\sum |\vec{p}_T \cdot \vec{n}_T|}{\sum p_T}$, where the sum runs over all charged particles, and the **thrust axis**, \vec{n}_T , maximizes the expression. For $n_{sel} \geq 2$.

The solution for \vec{n}_T is found iteratively: $\vec{n}_T^{(j+1)} = \frac{\sum \varepsilon(\vec{n}_T^{(j)} \cdot \vec{p}_T) \vec{p}_T}{|\sum \varepsilon(\vec{n}_T^{(j)} \cdot \vec{p}_T) \vec{p}_T|}$, where $\varepsilon(x > 0) = 1$ and $\varepsilon(x < 0) = -1$.

- **Spherocity:** $S = \frac{\pi^2}{4} \min_{\vec{n}=(n_x, n_y, 0)^T} \left(\frac{\sum |\vec{p}_T \times \vec{n}|}{\sum p_T} \right)^2$, where the sum runs over all charged particles and the vector \vec{n} minimizes the expression. For $n_{sel} \geq 2$.

- **The F -parameter** defined as the ratio of the smaller and larger **eigenvalues**, λ_1, λ_2 and $\lambda_1 \leq \lambda_2$, $F = \frac{\lambda_1}{\lambda_2}$ of the **transverse momentum tensor** $M^{lin} = \sum_i \frac{1}{p_{T,i}} \begin{pmatrix} p_{x,i}^2 & p_{x,i} p_{y,i} \\ p_{x,i} p_{y,i} & p_{y,i}^2 \end{pmatrix}$, where the sum runs over the charged particles in an event. For $n_{sel} \geq 2$.

- **Drell-Yan $Z \rightarrow l^+ l^-$ decay products removed before calculating**

- **Corrected distributions after Bayesian unfolding**

Transverse thrust T and Sphericity S

Graphical representation of the spatial orientation in the transverse plane of selected charged particles for *Spherical* and *Pencil-like* events.

The transverse momentum vectors of charged particles is shown as blue lines, the length of which indicate the p_T of the corresponding particle in GeV.

For *Pencil-like* events the Transverse thrust, T , (red) and Sphericity, S , (green) axes (dashed lines) are almost identical.

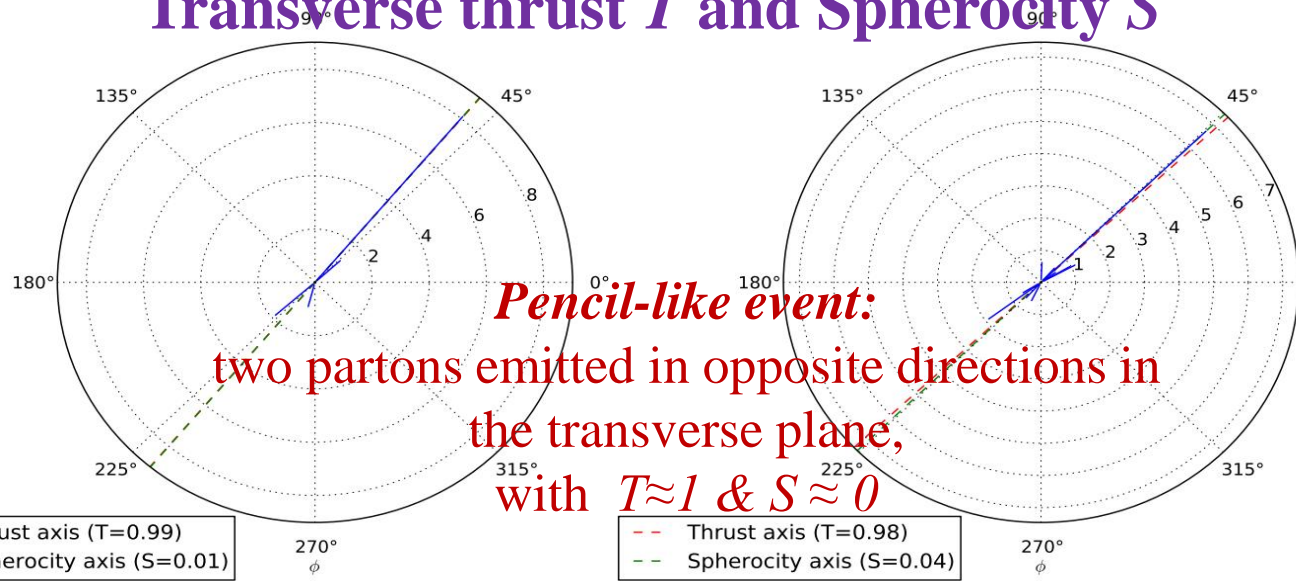
***Spherical event:* $T = 2/\pi$, $S \approx 1$, $F \approx 1$**

***Pencil-like event:* $T = 1$, $S \approx 0$, $F \approx 0$**

These observables are

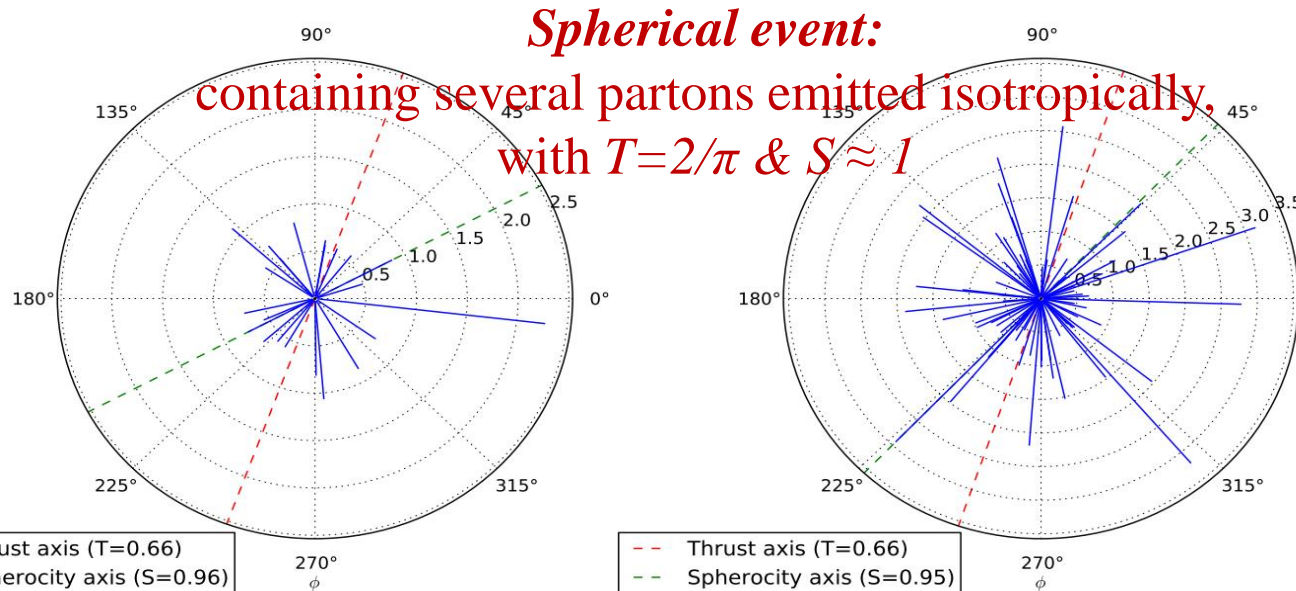
✓ **Very high correlated amongst themselves!**

✓ **Weakly correlated with N_{ch} , $\sum p_T$, B**



Pencil-like event:
two partons emitted in opposite directions in the transverse plane, with $T \approx 1$ & $S \approx 0$

(a) Pencil-like events



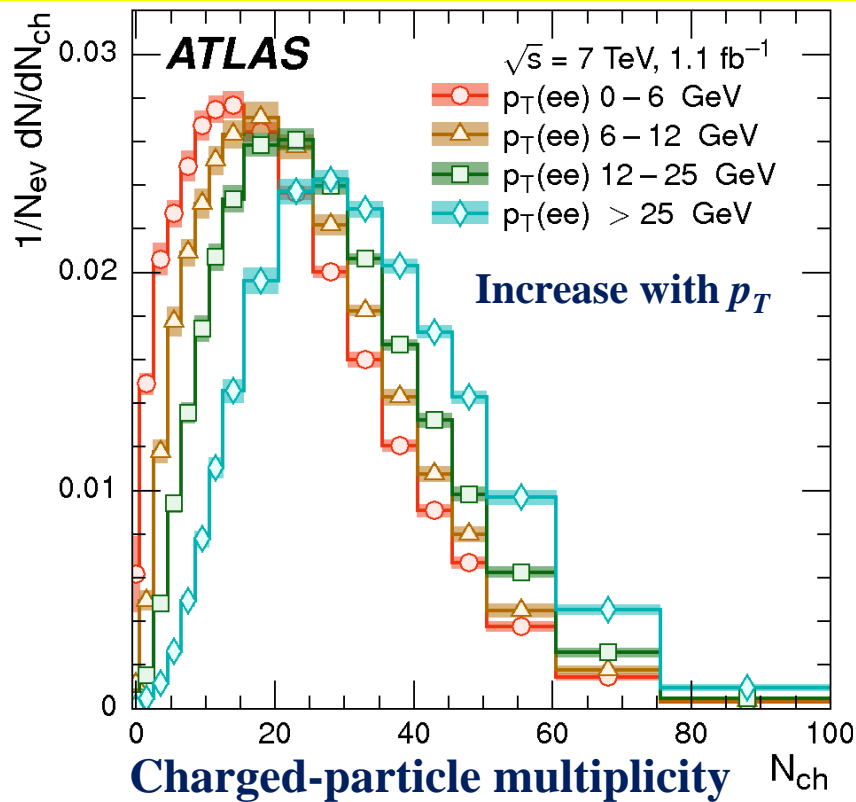
Spherical event:
containing several partons emitted isotropically, with $T = 2/\pi$ & $S \approx 1$

(b) Spherical events

<i>Observable</i>	δ_O^{stat} [%]	δ_O^{Lepton} [%]	$\delta_O^{Tracking}$ [%]	$\delta_O^{Non-Prim.}$ [%]	$\delta_O^{Pile-up}$ [%]	$\delta_O^{Multijet}$ [%]	δ_O^{Unfold} [%]	δ_O^{Total} [%]
\mathcal{N}_{ch}	1-5	0.2-0.6	<0.1-9	0.1-2.5	0.5-28	<0.1-0.6	0.2-8.4	0.6-28
Σp_T	1-3	0.1-0.5	0.3-5.5	<0.1-1.3	0.1-6.8	0.01-0.4	<0.1-0.8	0.1-9
\mathcal{B}	0.8-14	0.1-2.4	<0.1-6.2	0.1-2.1	0.1-36	<0.1-2.1	0.2-2.9	0.3-36
\mathcal{T}	0.6-4.4	0.1-0.5	0.2-2.2	0.1-1.6	0.1-4.7	0.1-0.3	0.1-2.6	0.3-5
\mathcal{S}	0.6-3.8	0.1-0.4	0.3-2.6	0.1-1.4	0.1-4.3	0.1-0.4	0.1-2.2	0.4-5
\mathcal{F}	0.6-3.6	0.1-0.5	0.3-1.6	0.1-1.5	0.1-1.7	0.1-0.3	0.1-2.0	0.4-3

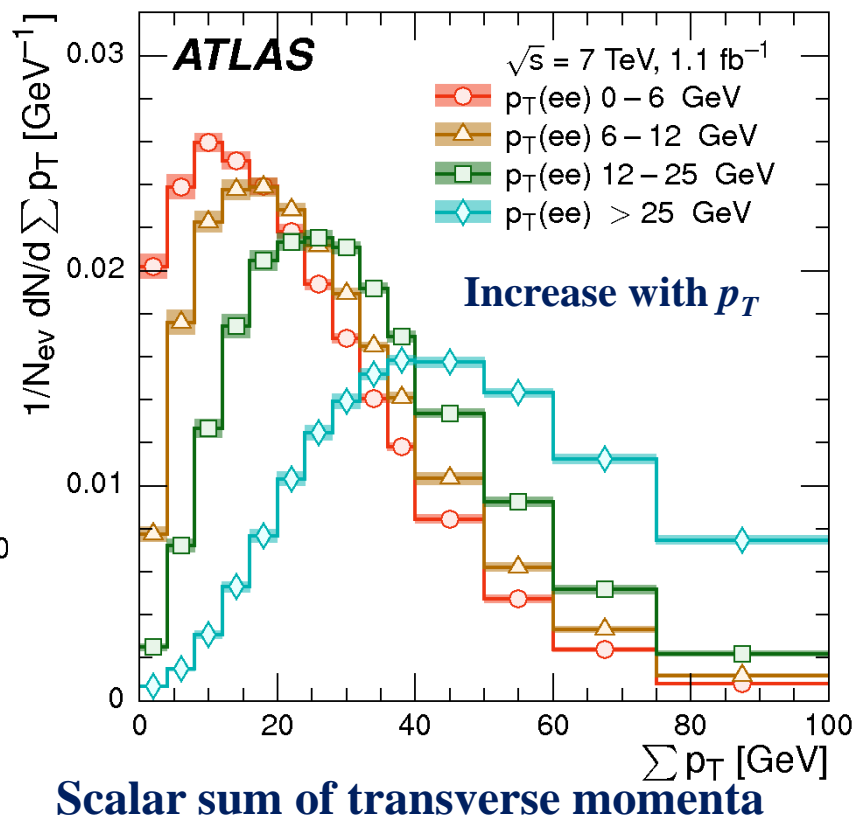
Ranges of the relative uncertainties δ_O/O of the event-shape observables O for the electron channels (e^+e^-) for the $p_T(e^+e^-)$ range 0 – 6 GeV in percent.

The systematic uncertainties are dominated.

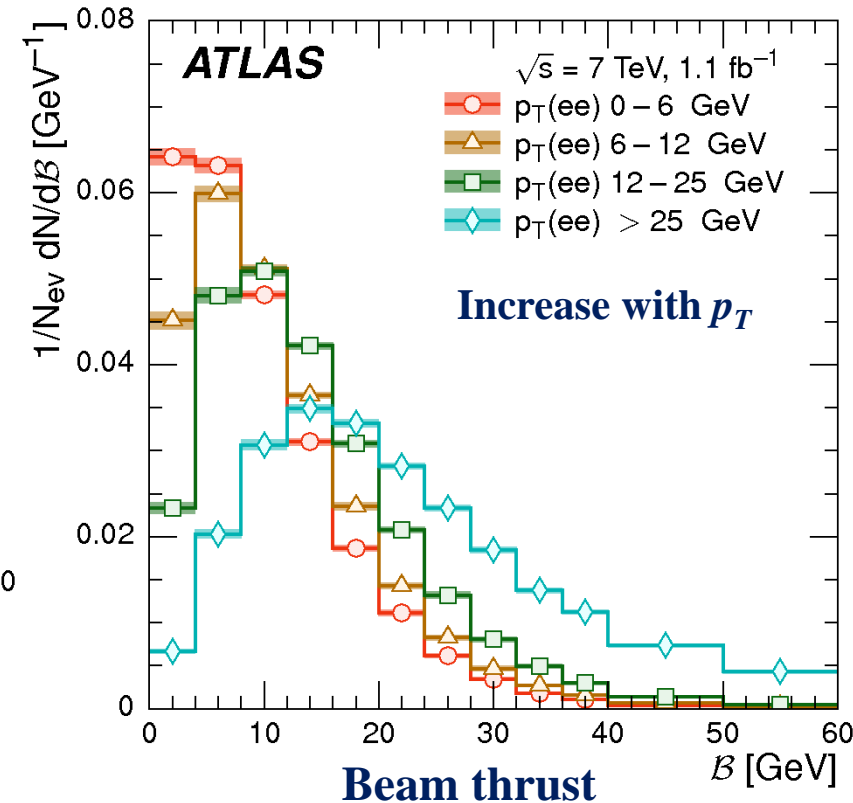


Event-shape distributions in $Z \rightarrow e^+e^-$

Recoiling Jet emerging for higher $p_T(e^+e^-)$



Similar distributions for $Z \rightarrow \mu^+ \mu^-$

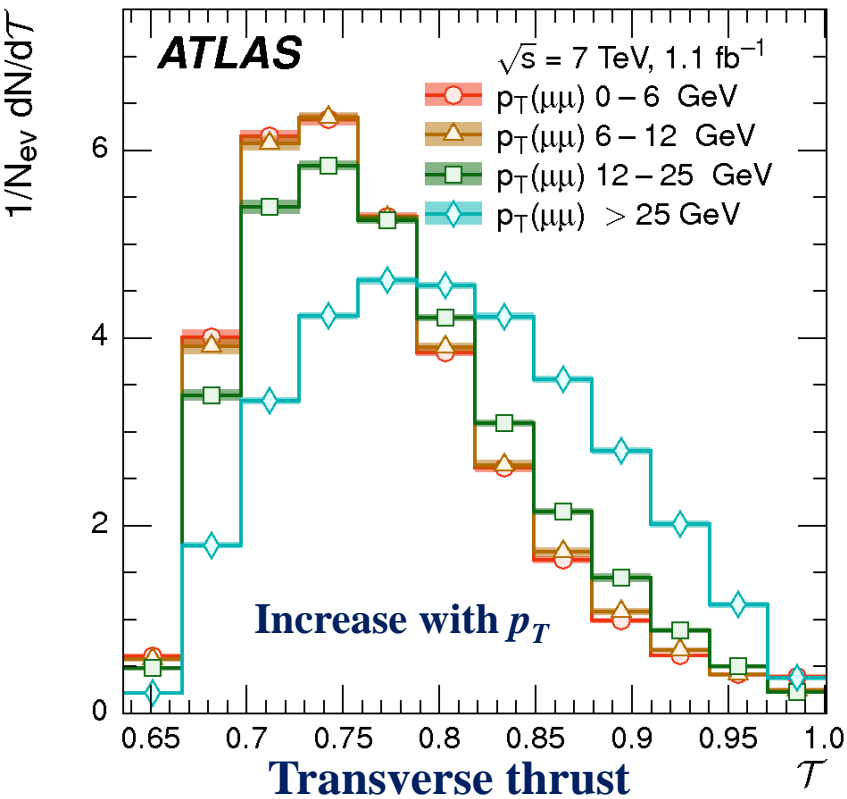


$$B = \sum p_T e^{-|\eta|}$$

4 phase-space regions:

- $p_T(\ell) < 6 \text{ GeV}$
- $p_T(\ell) = 6 - 12 \text{ GeV}$
- $p_T(\ell) = 12 - 25 \text{ GeV}$
- $p_T(\ell) > 25 \text{ GeV}$

The unfolded electron channel results for the observables in the various $p_T(e^+e^-)$ ranges, with the total uncertainty presented as the quadratic sum of the statistical and total systematic uncertainties.



$$T = \max_{\vec{n}_T} \frac{\sum |\vec{p}_T \cdot \vec{n}_T|}{\sum p_T}$$

4 phase-space regions:

$p_T(\ell\ell) < 6$ GeV

$p_T(\ell\ell) = 6 - 12$ GeV

$p_T(\ell\ell) = 12 - 25$ GeV

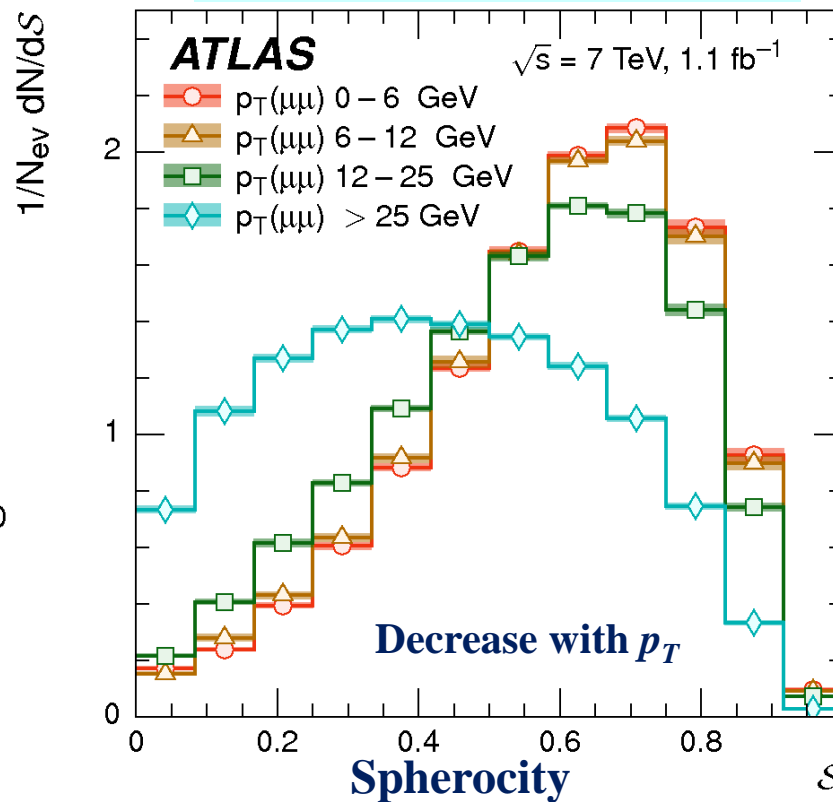
$p_T(\ell\ell) > 25$ GeV

Yuri Kulchitsky

The unfolded muon channel results for the observables in the various $p_T(\mu^+\mu^-)$ ranges, with the total uncertainty presented as the quadratic sum of the statistical and total systematic uncertainties.

Event-shape distributions for $Z \rightarrow \mu^+\mu^-$

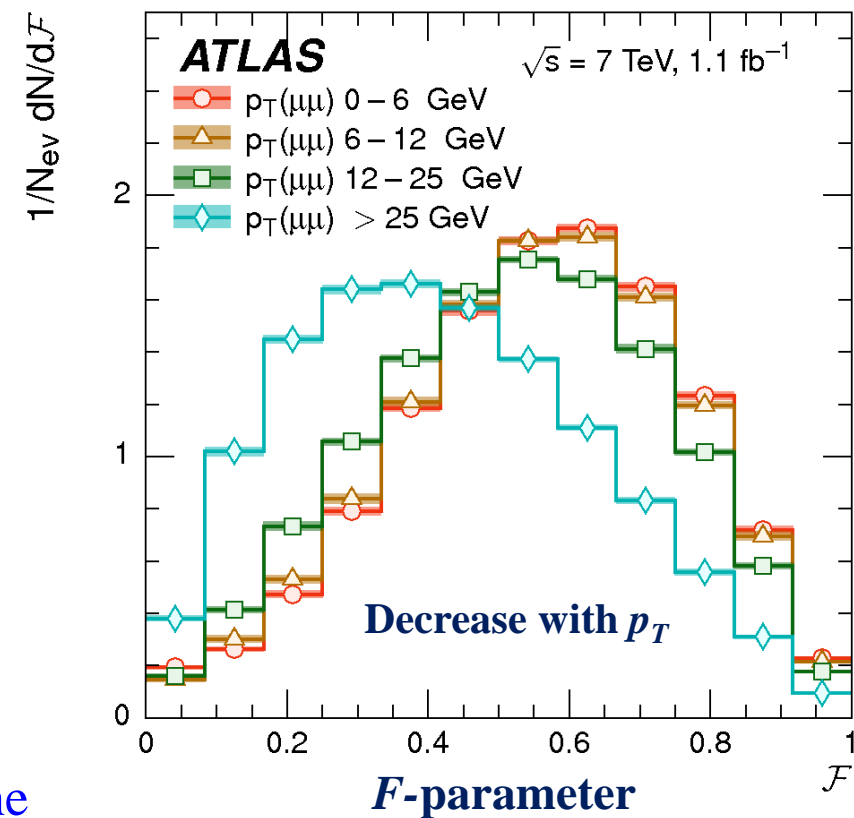
$$S = \frac{\pi^2}{4} \min_{\vec{n}=(n_x, n_y, 0)^T} \left(\frac{\sum |\vec{p}_T \times \vec{n}_T|}{\sum p_T} \right)^2$$



Decrease with p_T

Recoiling Jet emerging for higher $p_T(\mu^+\mu^-)$

Similar distributions for $Z \rightarrow e^+e^-$



Decrease with p_T

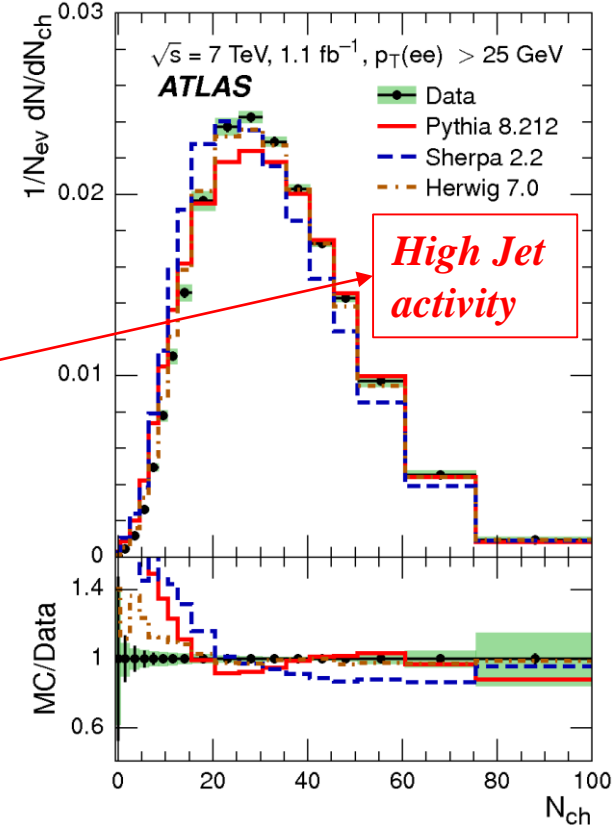
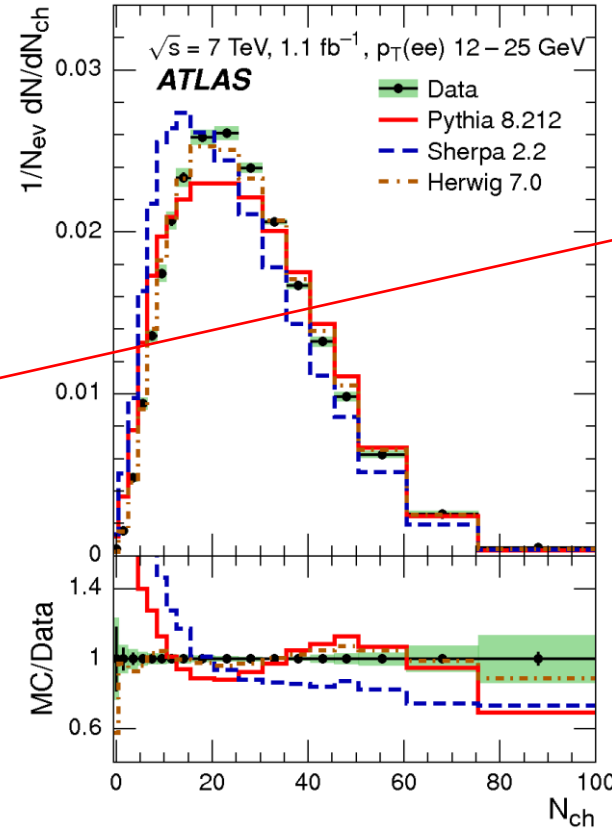
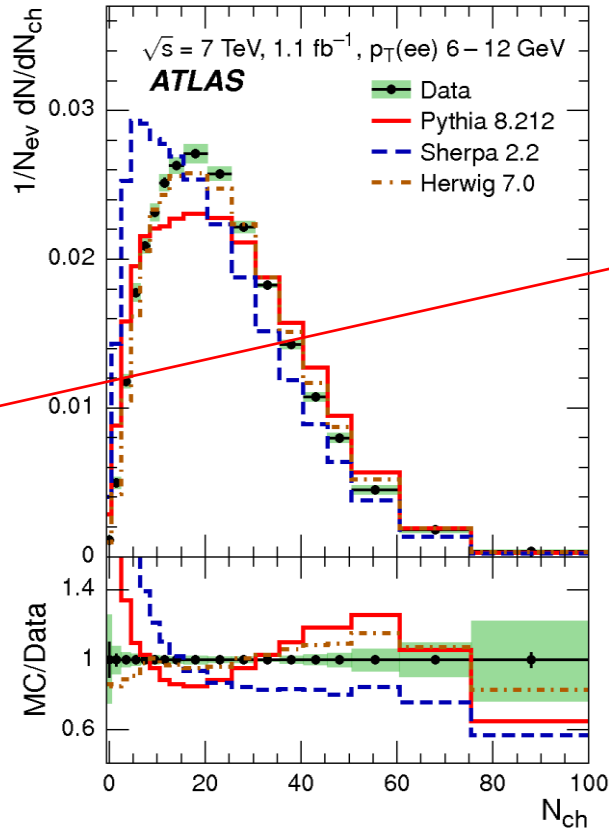
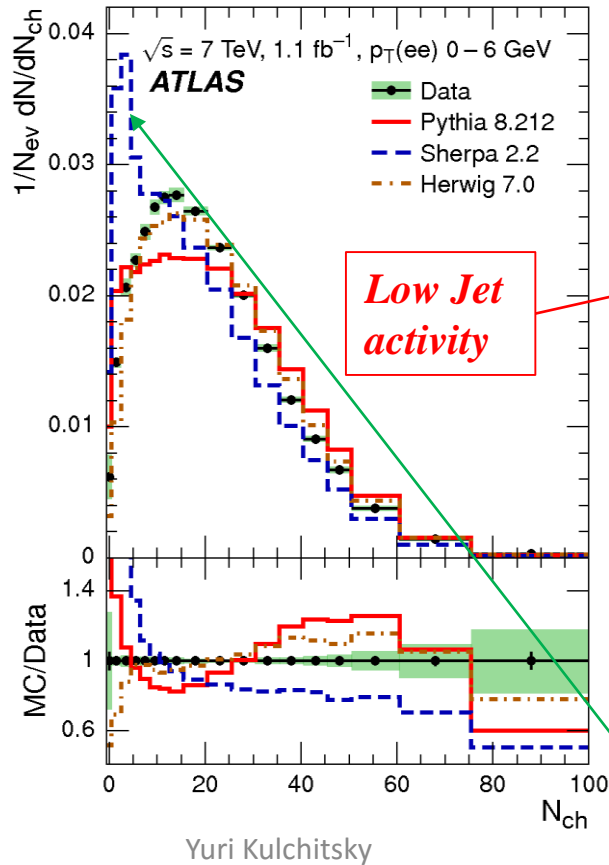
$$F = \frac{\lambda_1}{\lambda_2}$$

$$\frac{1}{N_{ev}} \frac{dN}{dN_{ch}} \text{ vs. } N_{ch}$$

Event-shape distributions in $Z \rightarrow e^+e^-$

Similar distributions for $Z \rightarrow \mu^+\mu^-$

Underline Event sensitively region



For $p_T > 25 \text{ GeV}$ - at least one high jet recoiling against the Z

Best agreement for Pythia, Herwig and Sherpa at large p_T

Distribution of charged-particle multiplicity, N_{ch} , for $Z \rightarrow e^+e^-$ for the four $p_T(e^+e^-)$ ranges: 0-6, 6-12, 12-25, $\geq 25 \text{ GeV}$ compared to the predictions Pythia8, Sherpa, and Herwig7.

Event-shape observables *Scalar sum of transverse momenta* in $Z \rightarrow \mu^+\mu^-$ for p_T regions

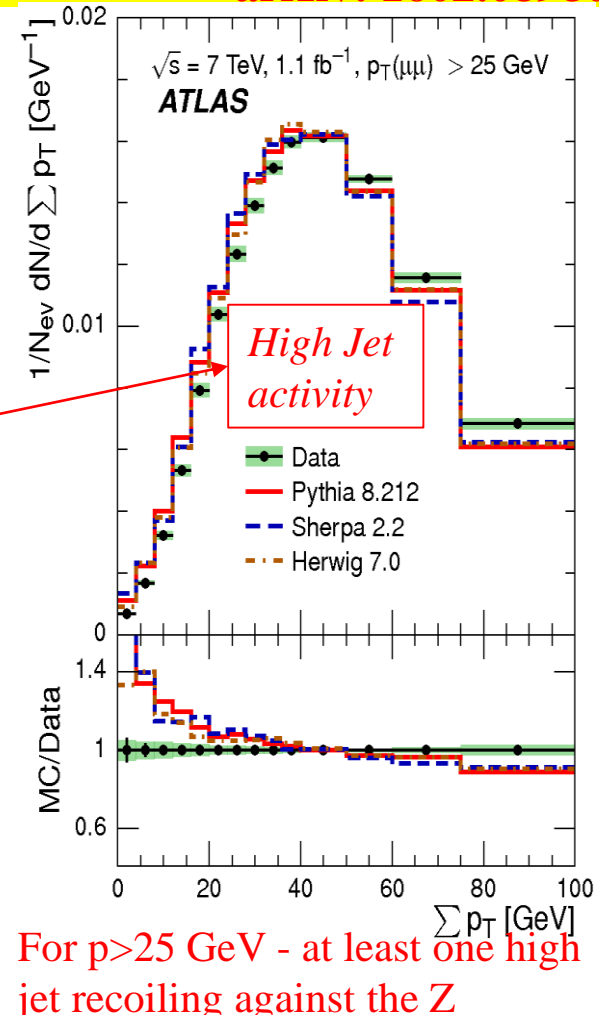
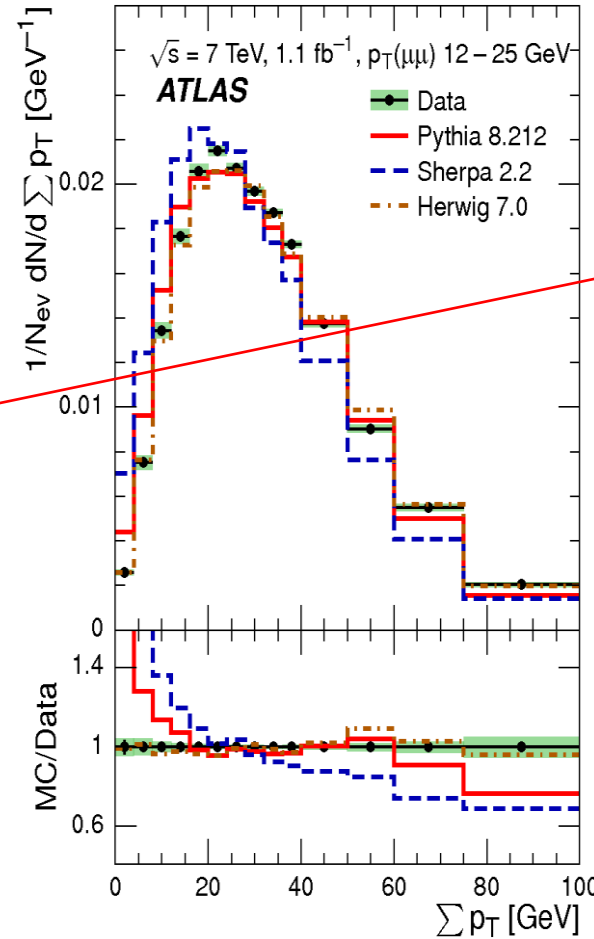
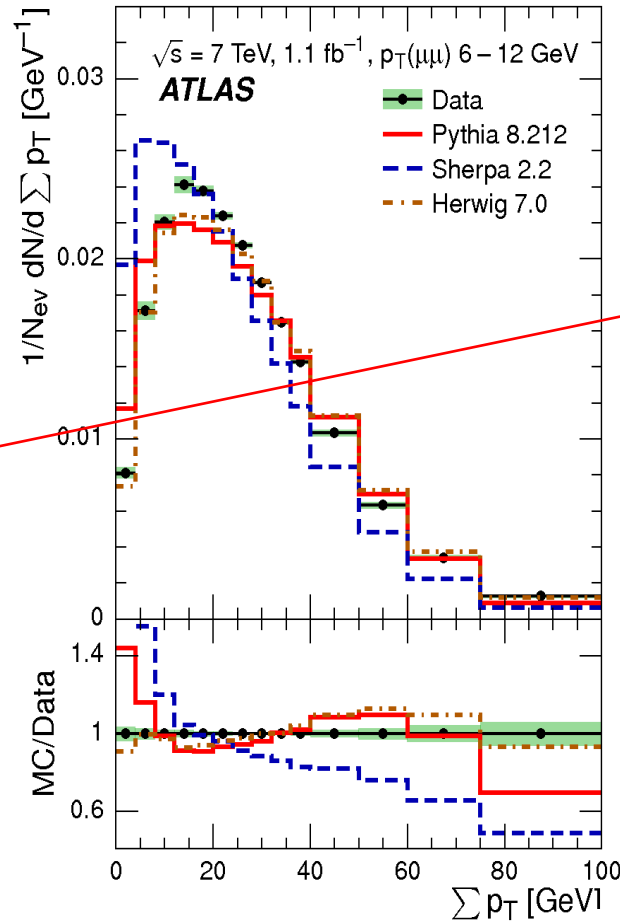
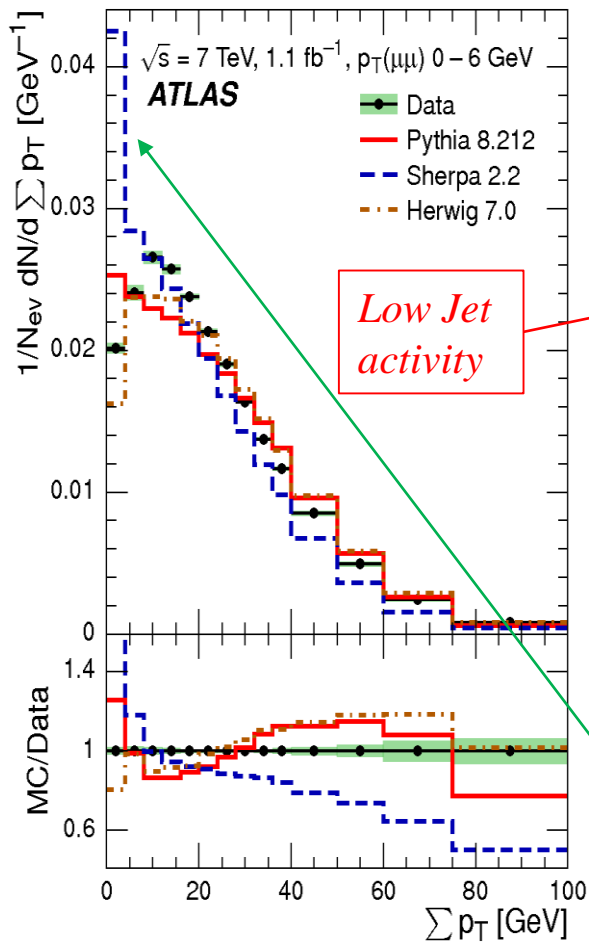
arXiv: 1602.08980

$$\frac{1}{N_{ev}} \frac{dN}{d\sum p_T} \text{ vs. } \sum p_T$$

Event-shape distributions in $Z \rightarrow \mu^+\mu^-$

Similar distributions for $Z \rightarrow e^+e^-$

Underline Event sensitively region



For $p > 25$ GeV - at least one high jet recoiling against the Z

Best agreement for Pythia, Herwig and Sherpa at large p_T

Larger deviations with Sherpa at low p_T

Summed transverse momenta $\sum p_T$ for $Z \rightarrow \mu^+\mu^-$ for the four $p_T(\mu^+\mu^-)$ ranges: 0-6, 6-12, 12-25, ≥ 25 GeV compared to the predictions Pythia8, Sherpa, and Herwig7.

Event-shape observable *Beam thrust* in $Z \rightarrow \mu^+\mu^-$ for p_T regions

arXiv: 1602.08980

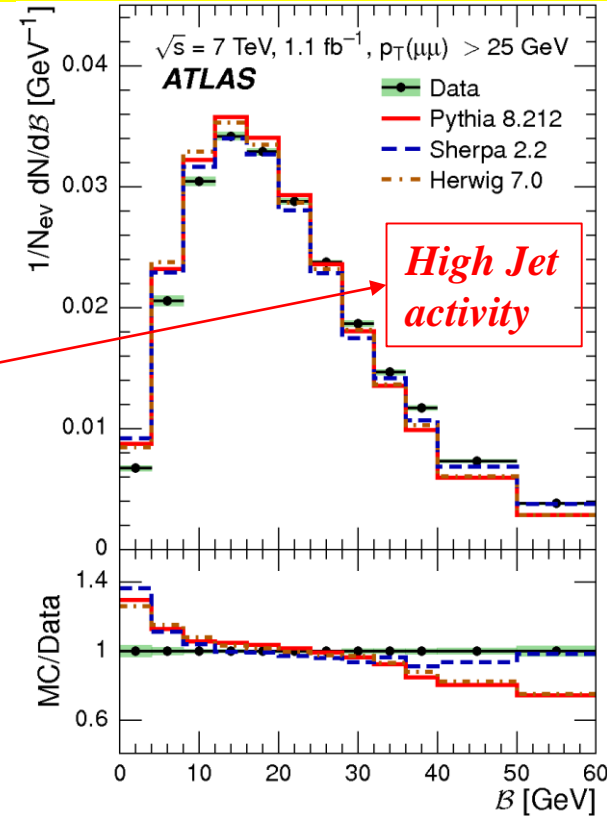
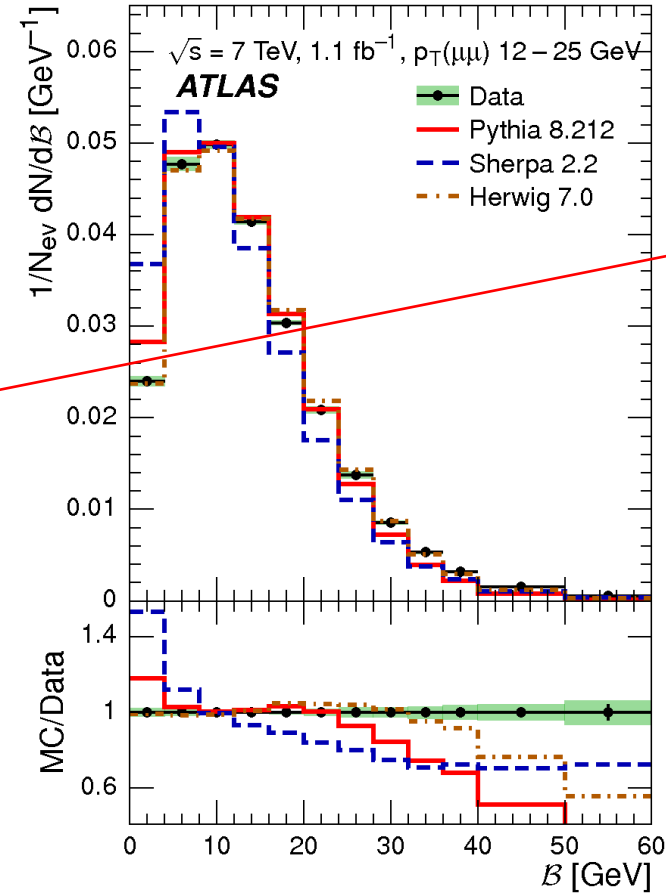
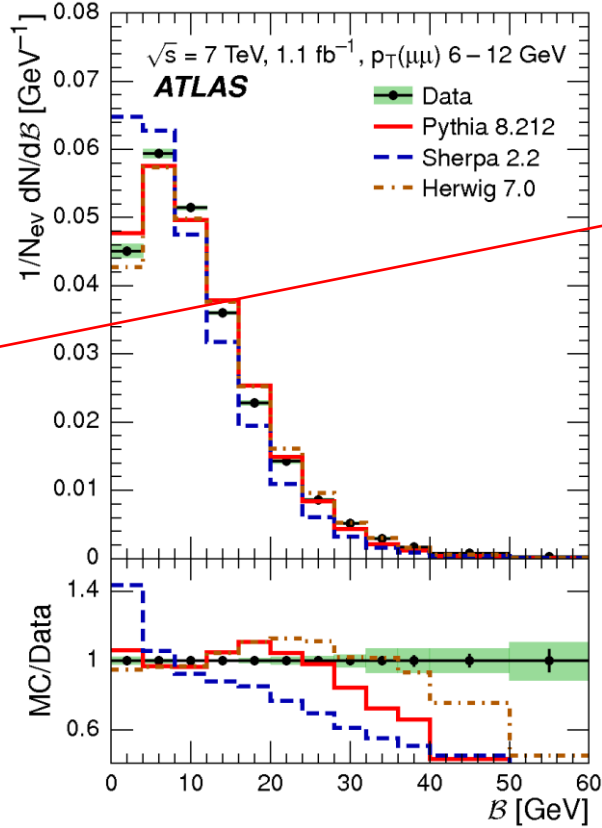
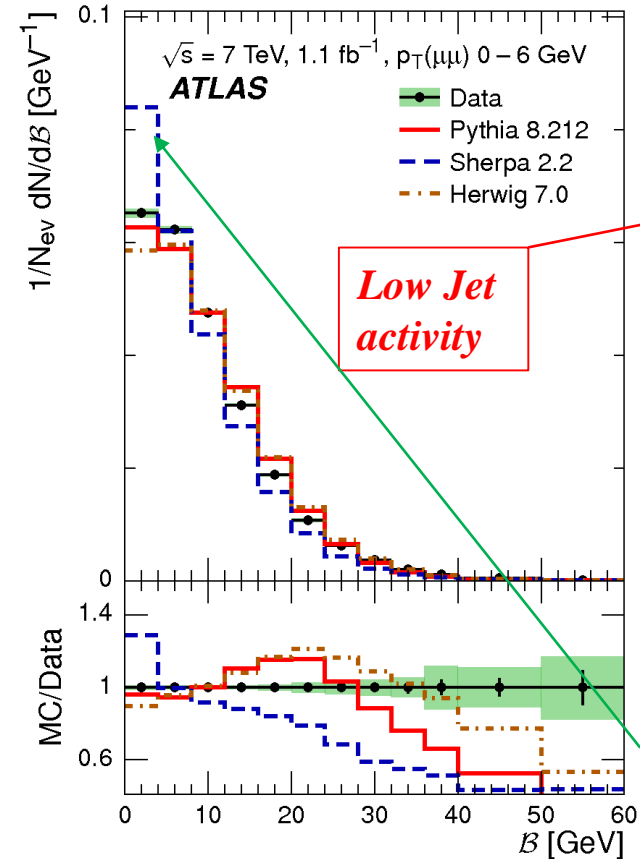
$$\frac{1}{N_{ev}} \frac{dN}{dB} \text{ vs. } B,$$

$$B = \sum p_T e^{-|\eta|}$$

Event-shape distributions for $Z \rightarrow \mu^+\mu^-$

Similar distributions are for $Z \rightarrow e^+e^-$

Underline Event sensitively region



Larger deviations with Sherpa at low p_T

Best agreement for Pythia, Herwig and Sherpa at large p_T

The best agreement is observed for Herwig7. Pythia8 still performs better than Sherpa.

Beam thrust, B , for $Z \rightarrow e^+e^-$ for the four $p_T(e^+e^-)$ ranges: 0-6, 6-12, 12-25, ≥ 25 GeV compared to the predictions Pythia8, Sherpa, and Herwig7.

Event-shape observable *Transverse thrust* in $Z \rightarrow e^+e^-$ for p_T regions

arXiv: 1602.08980

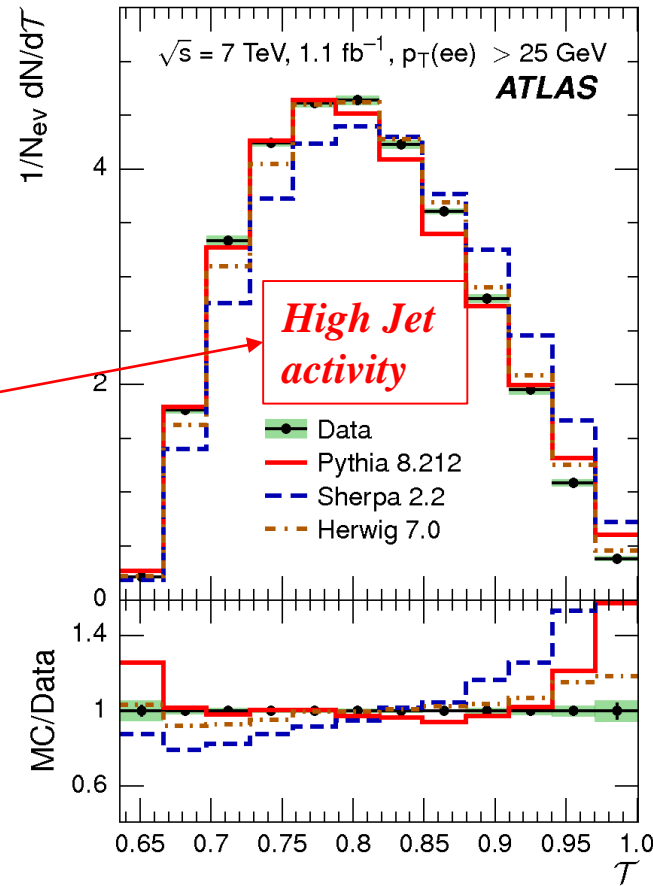
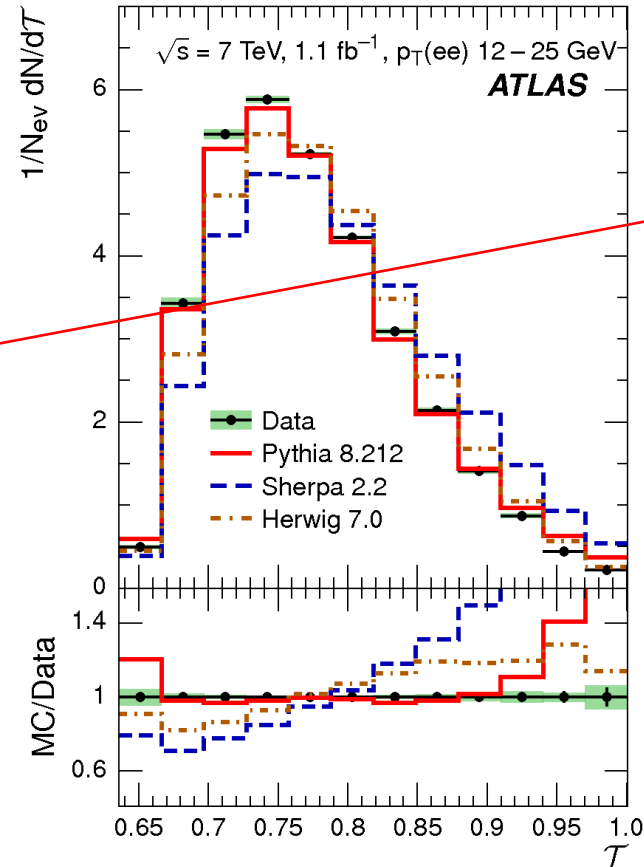
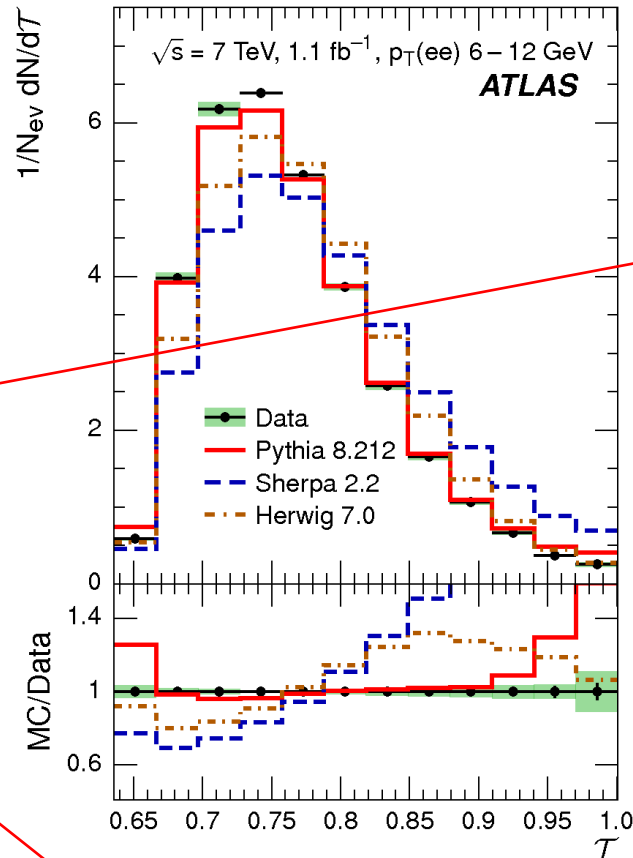
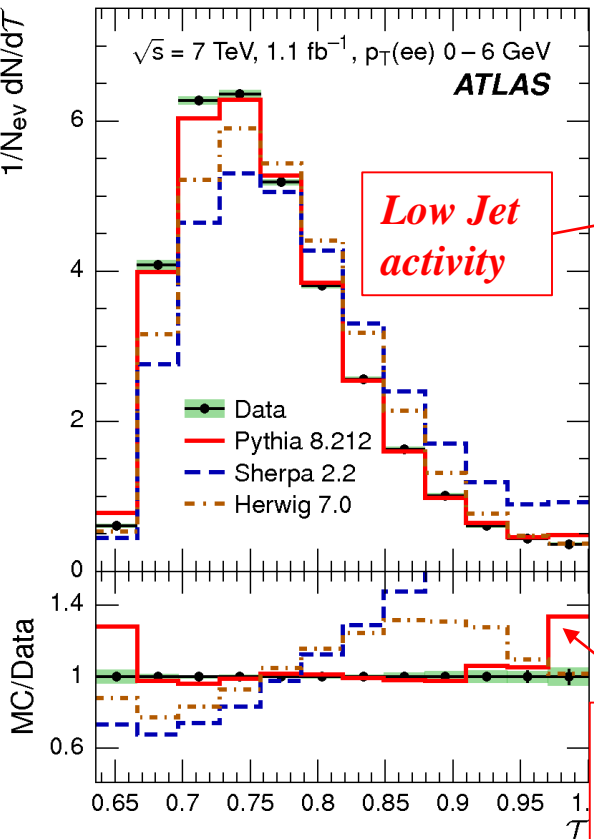
$$\frac{1}{N_{ev}} \frac{dN}{dT} \text{ vs. } T$$

$$T = \max_{\vec{n}_T} \frac{\sum |\vec{p}_T \cdot \vec{n}_T|}{\sum p_T}$$

Event-shape distributions in $Z \rightarrow e^+e^-$

Similar distributions for $Z \rightarrow \mu^+\mu^-$

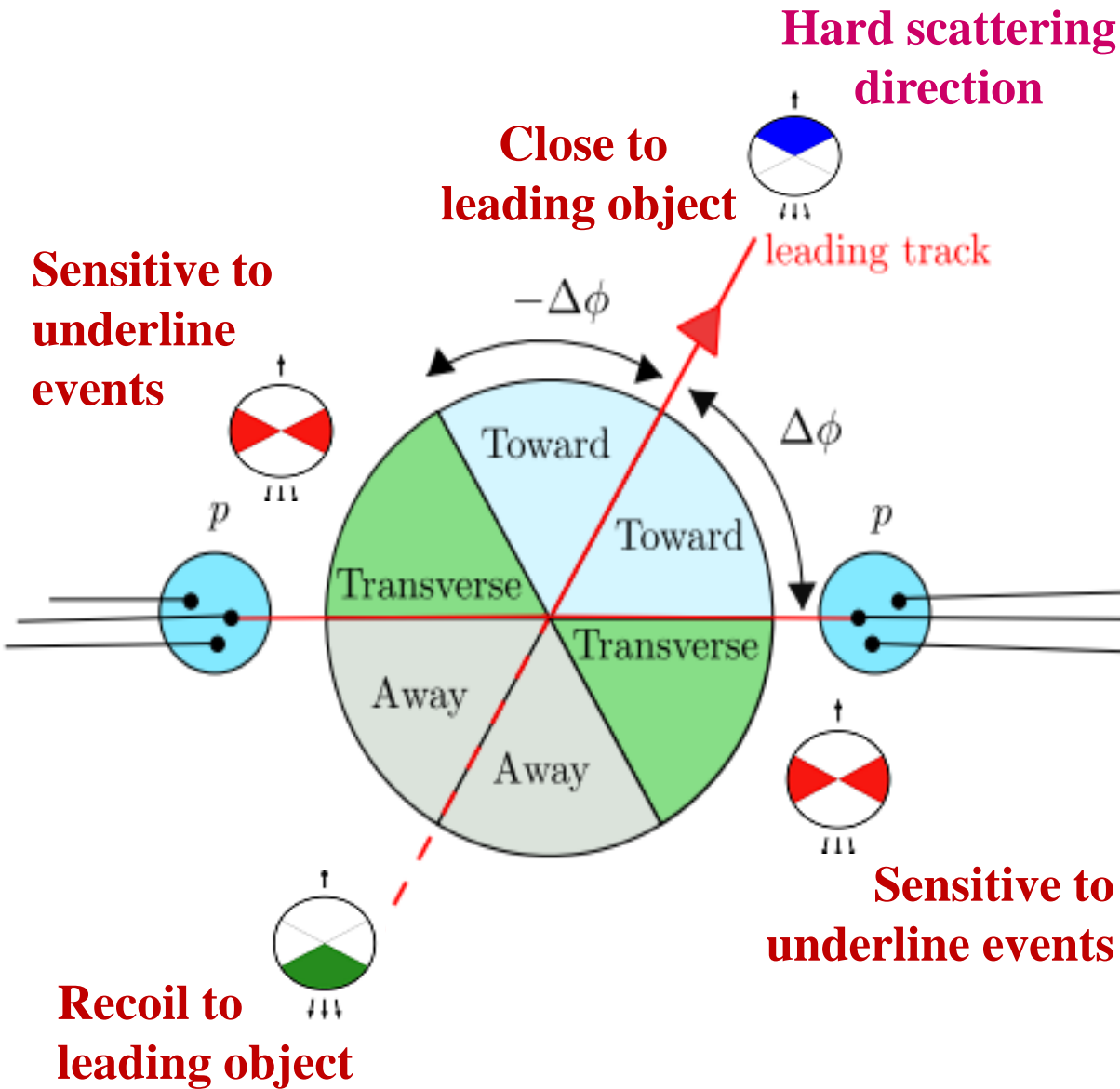
Underline Event sensitively region



Pythia8 very good agreement: for observables that are not very sensitive to the number of charged particles

Best agreement for Pythia, Herwig and Sherpa at large p_T

Transverse thrust, T , for $Z \rightarrow e^+e^-$ for the four $p_T(e^+e^-)$ ranges: 0-6, 6-12, 12-25, ≥ 25 GeV compared to the predictions Pythia8, Sherpa, and Herwig7.



Preliminary 13 TeV analysis based on *Leading track*:

- ▶ Same dataset and same event and track selection as the MB@13 analysis (see [Valentina Cairo report](#)) with *an additional requirement*: Leading track with $p_T \geq 1$ GeV
- ▶ Results presented at detector level, without any correction (the width of the vertex distribution along the Z axis in MC is reweighted to match the data)
- ▶ The tracking efficiency uncertainty is about $\leq 2\%$
- ▶ No correction for secondary tracks is performed

The data are compared with the Monte Carlo event generator predictions, after passing the generated events through the ATLAS detector simulation, which is based on Geant 4.

Generator	Version	Tune	PDF	Focus of Tune
Pythia8	8.186	A2	MSTW2008LO	MB
Pythia8	8.186	Monash	NNPDF2.3LO	MB/UE
Pythia8	8.186	A14	NNPDF2.3LO	UE/Shower
Herwig++	2.7.1	UEEE5	CTEQ6L1	UE
Epos	3.1	LHC		MB

The tunes use data from different experiments to constrain different processes.

Some tunes are focused on describing the **MB** distributions better.

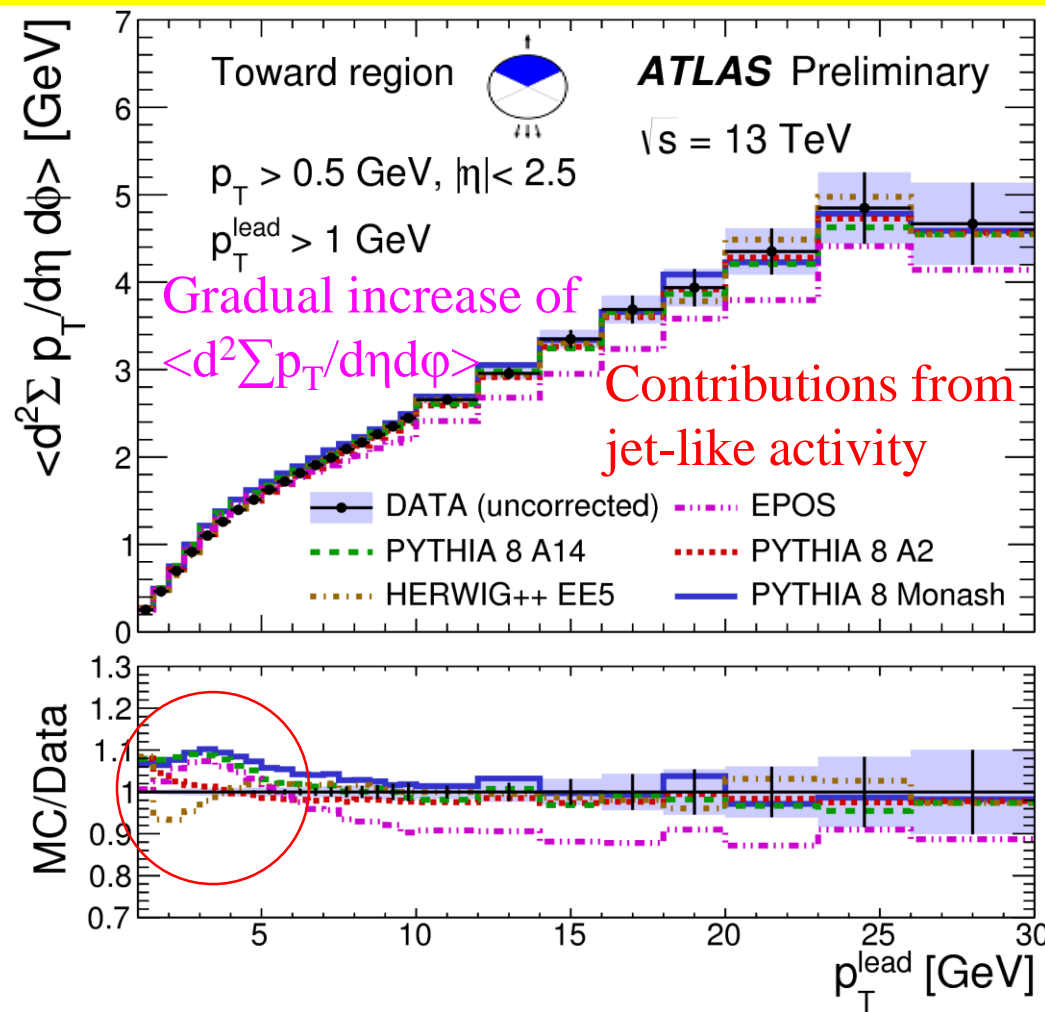
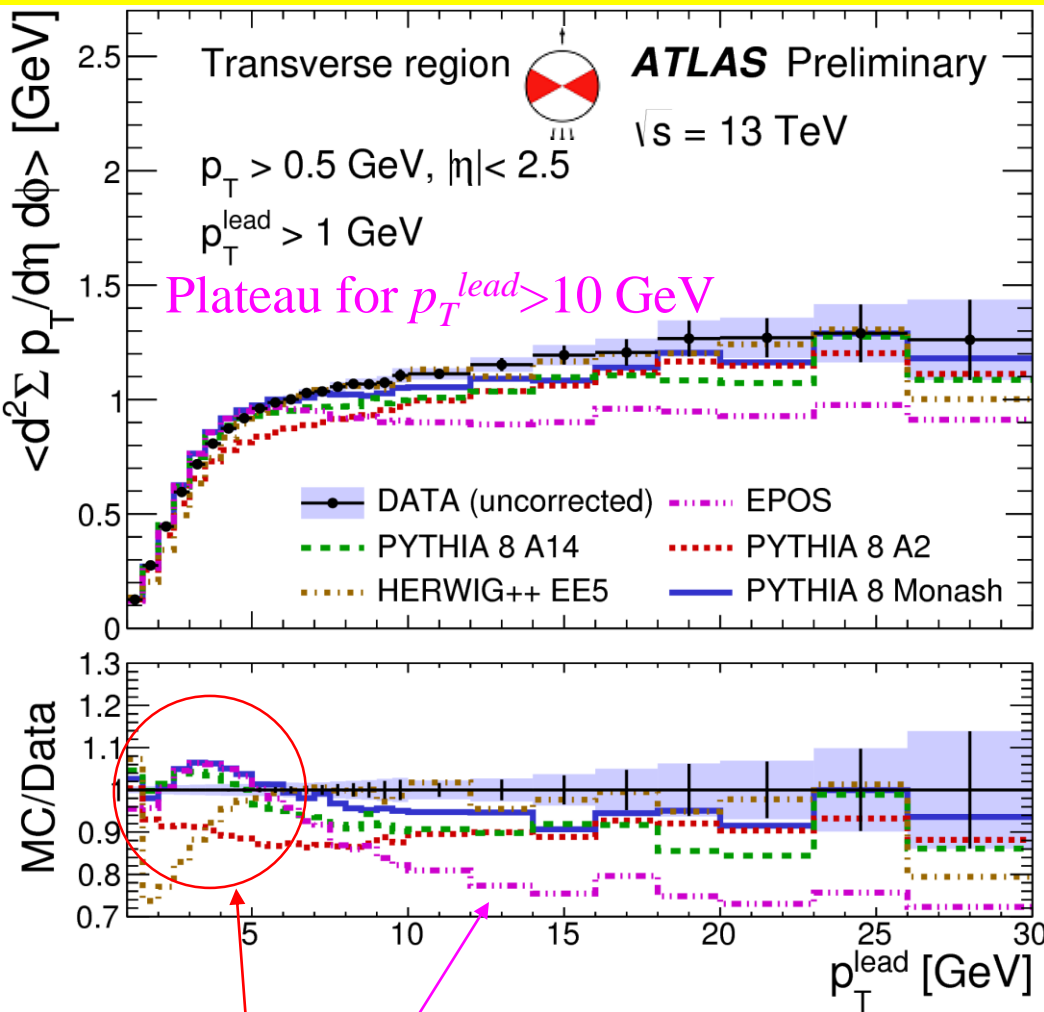
The rest models are tuned to describe the **UE** distributions.

Definition of the measured observables

Observable	Name	Definition
$\langle d^2N_{ch}/d\eta d\phi \rangle$	Average track multiplicity density	Number of tracks per unit $\eta-\phi$
$\langle d^2\sum p_T/d\eta d\phi \rangle$	Average scalar p_T sum density	Scalar sum of track p_T per unit $\eta-\phi$

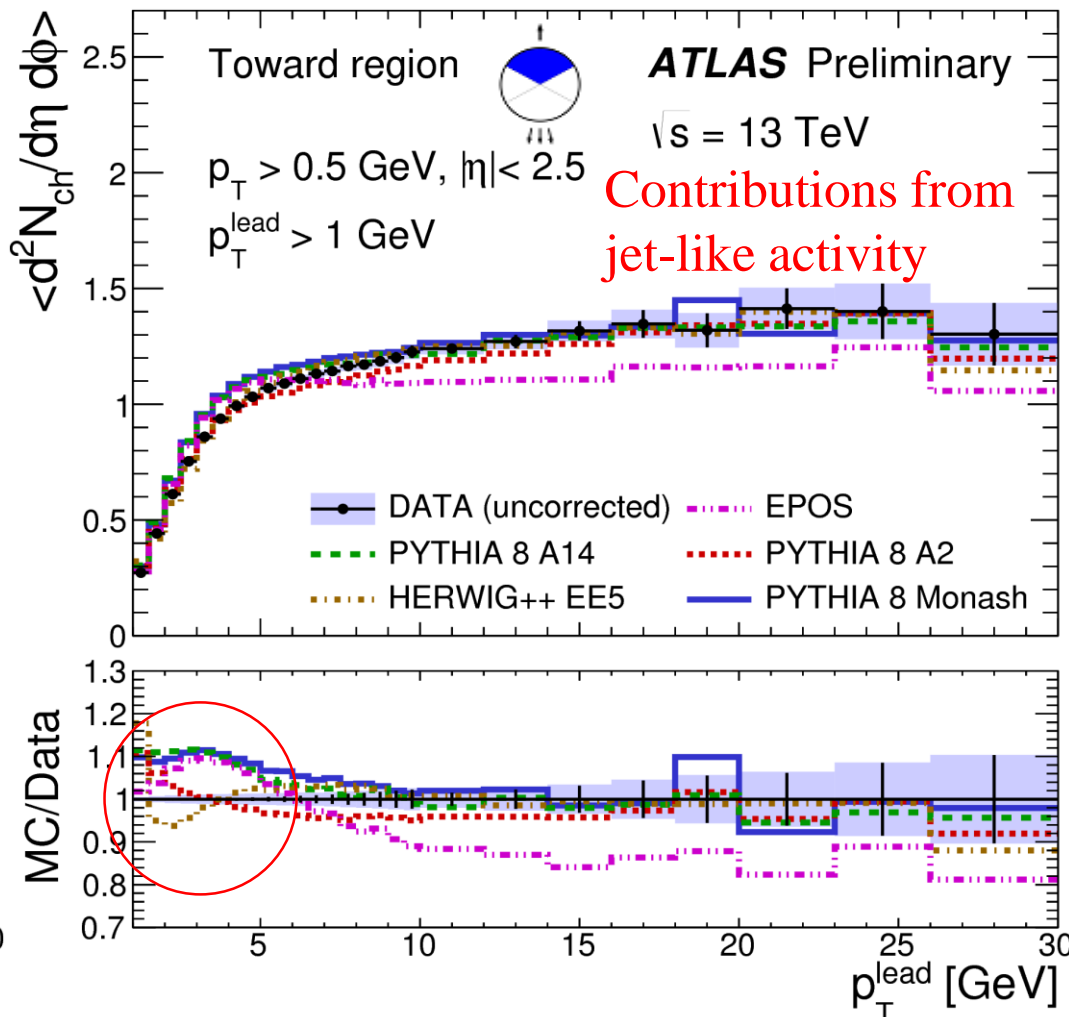
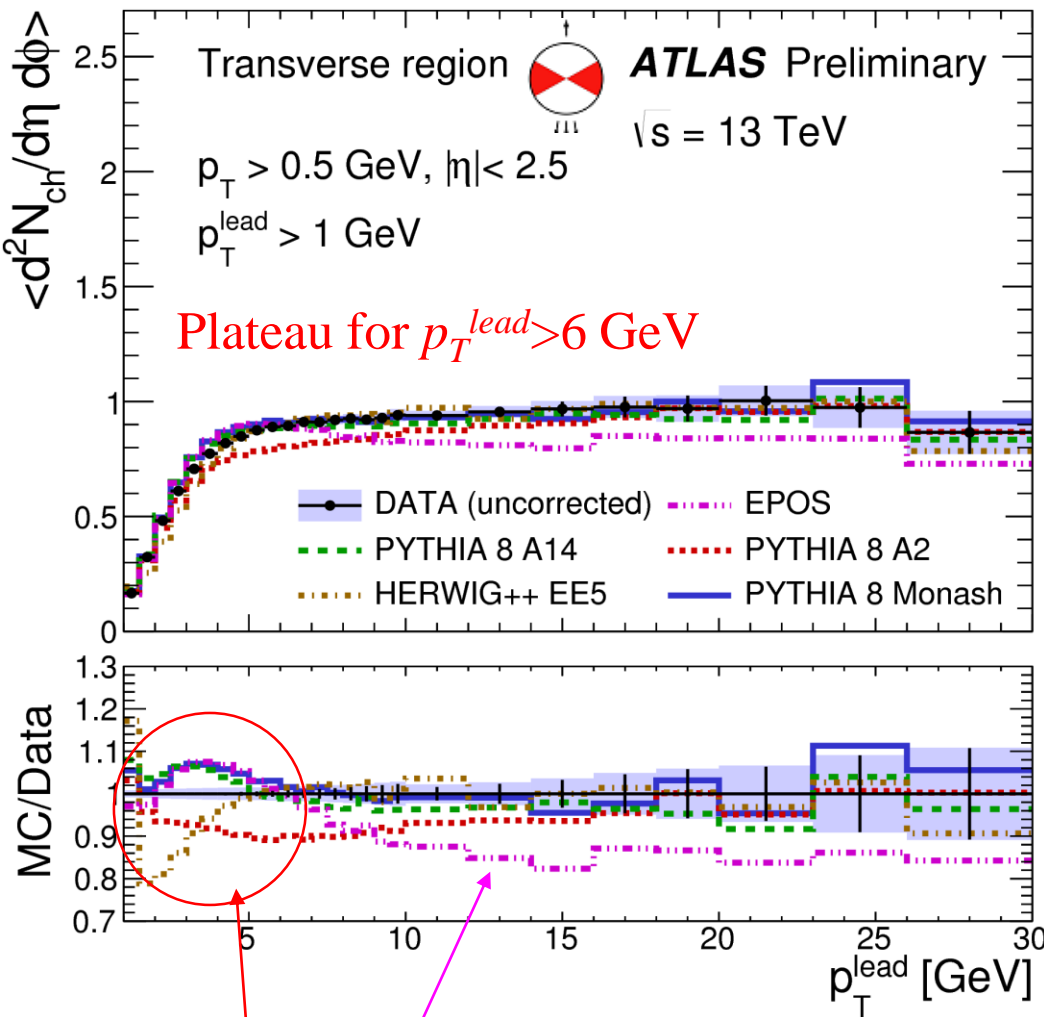
Distributions of *average scalar p_T sum* vs p_T^{lead} at 13 TeV

ATL-PHYS-PUB-2015-019



Comparison of detector level data and MC predictions for average scalar p_T sum density of tracks as a function of track p_T^{lead} in the transverse (left) and toward (right) regions.

- ▶ From 10 GeV: Good description for the UE tunes (Herwig++, Pythia A14, Monash)
- ▶ None of the MC models describe the initial rise well
- ▶ The EPOS 20% off in the plateau (indicated the absence of semi-hard minimum-bias events)

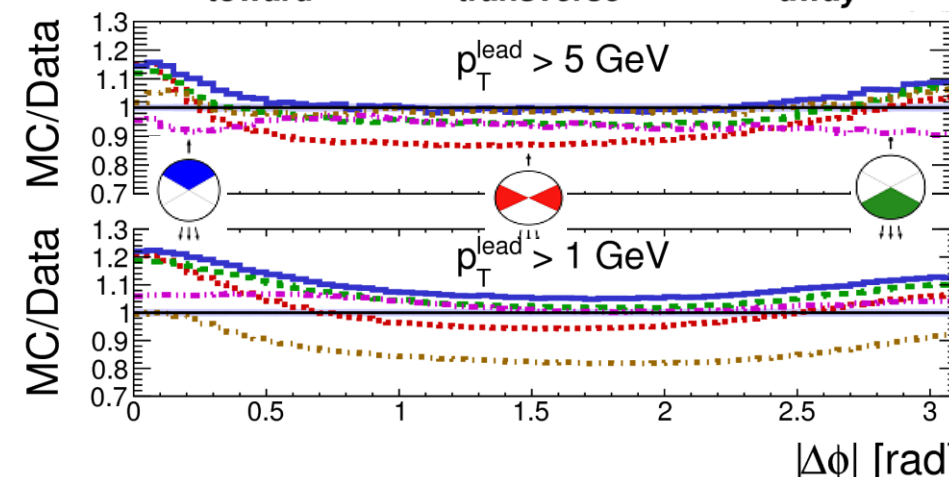
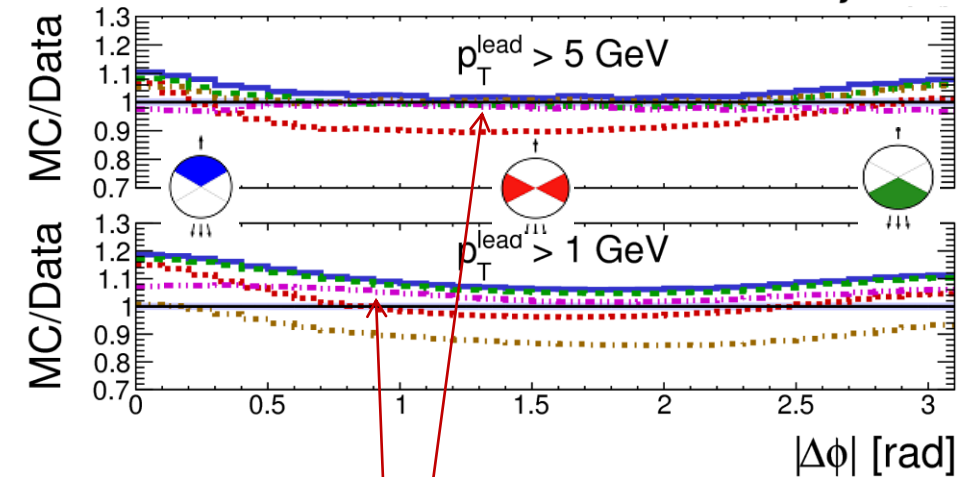
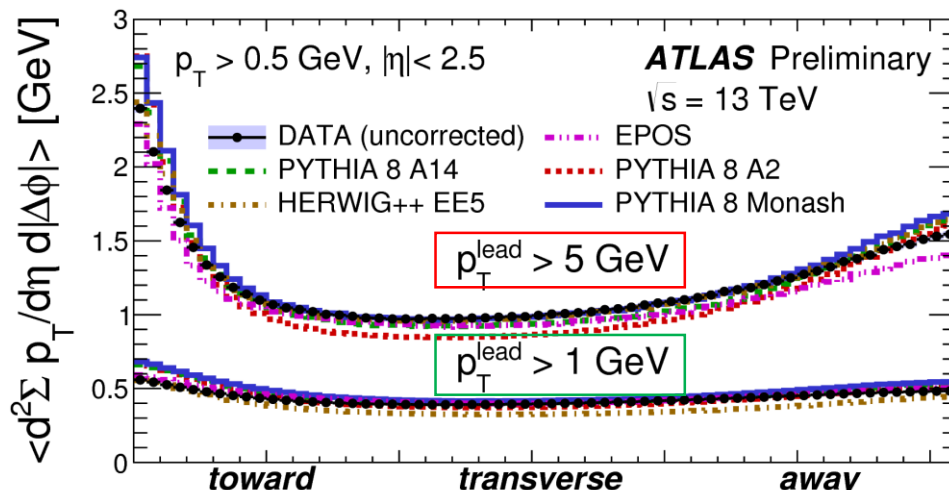
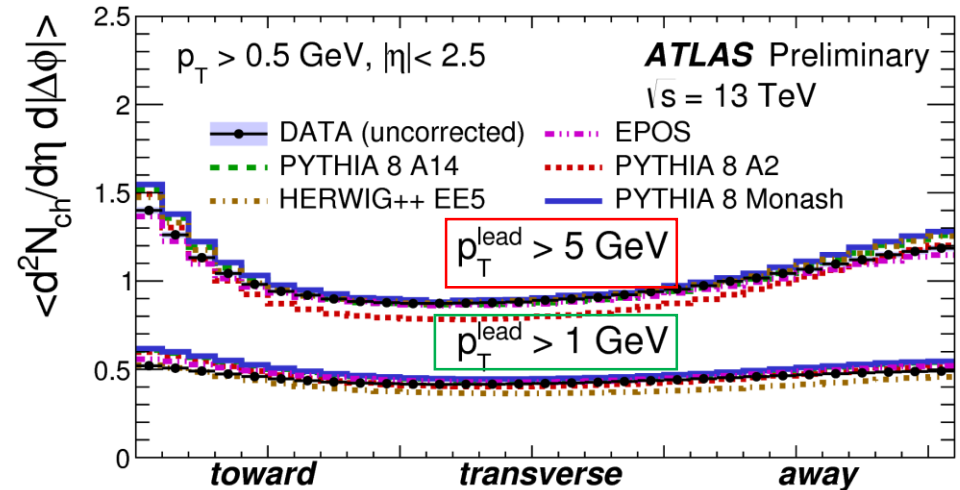


Comparison of detector level data and MC predictions for average track multiplicity density values as a function of track p_T^{lead} in the transverse (left) and toward (right) regions.

- ▶ Good prediction of Herwig++ & Pythia A14, Monash in the **plateau** part of Transverse region
- ▶ None of the MC models describe the initial rise well
- ▶ The **EPOS** predicts significantly less ($\sim 15\%$) activity at higher p_T^{lead}

Distributions of *average track multiplicity and p_T sum* vs $|\Delta\phi|$

ATL-PHYS-PUB-2015-019



Comparison of detector level data and MC predictions for the $|\Delta\phi|$ distributions of average track multiplicity density (left) and average scalar p_T sum density of tracks (right).

The leading track is defined to be at $\Delta\phi=0$, and excluded from the distributions.

- ▶ For $p_T^{\text{lead}} > 1 \text{ GeV}$: Good agreement with MB tune (Pythia A2, EPOS)
- ▶ For $p_T^{\text{lead}} > 5 \text{ GeV}$: Good agreement with UE tunes (Herwig++, Pythia Monash, Pythia A14)
- ▶ The distributions do not show a significant difference between Data and MC predictions

Summary

- **The event-shape observables sensitive to the underlying event** were measured in 1.1 fb^{-1} integrated luminosity of pp collisions at $\sqrt{s} = 7 \text{ TeV}$. Events with an invariant mass close to the Z-boson mass ($Z \rightarrow e^+e^-$ and $Z \rightarrow \mu^+\mu^-$) were selected.
- The *charged particle multiplicity, mean transverse momentum, Beam thrust, Transverse thrust, Sphericity, and F-parameter* were measured.
- The resulting distributions are presented in different regions of the Z-boson p_T and compared to predictions of the MC event generators, which provide predictions that are in better agreement with the data at high Z-boson transverse momenta than at low Z-boson transverse momenta.
- **Underlying event analysis at $\sqrt{s} = 13 \text{ TeV}$** data are shown: reasonable agreement of tunes used in Atlas MC with new data. The data sample corresponds to an integrated luminosity of $151 \mu\text{b}^{-1}$. These detector level distributions show discriminating power between different MC models.

**MANY THANKS TO YOU
FOR ATTENTION!**

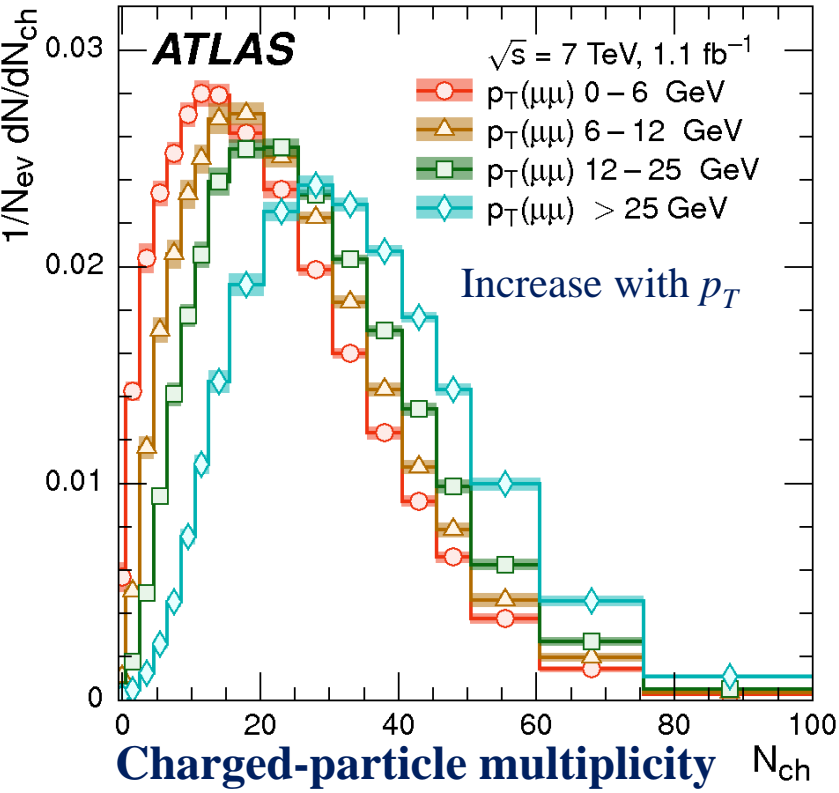
BACKUP SLIDES

Publications

- ATLAS Collaboration, *Measurement of event-shape observables in $Z \rightarrow l^+l^-$ events in pp collisions at $\sqrt{s}=7$ TeV with the ATLAS detector at the LHC*; arXiv:1602.08980 [hep-ex], CERN-EP-2016-015; <http://cds.cern.ch/record/2134966>
- ATLAS Collaboration, *Detector level leading track underlying event distributions at 13 TeV measured in ATLAS*; ATL-PHYS-PUB-2015-019, CERN, Geneva, July 2015; <http://cds.cern.ch/record/2037684>

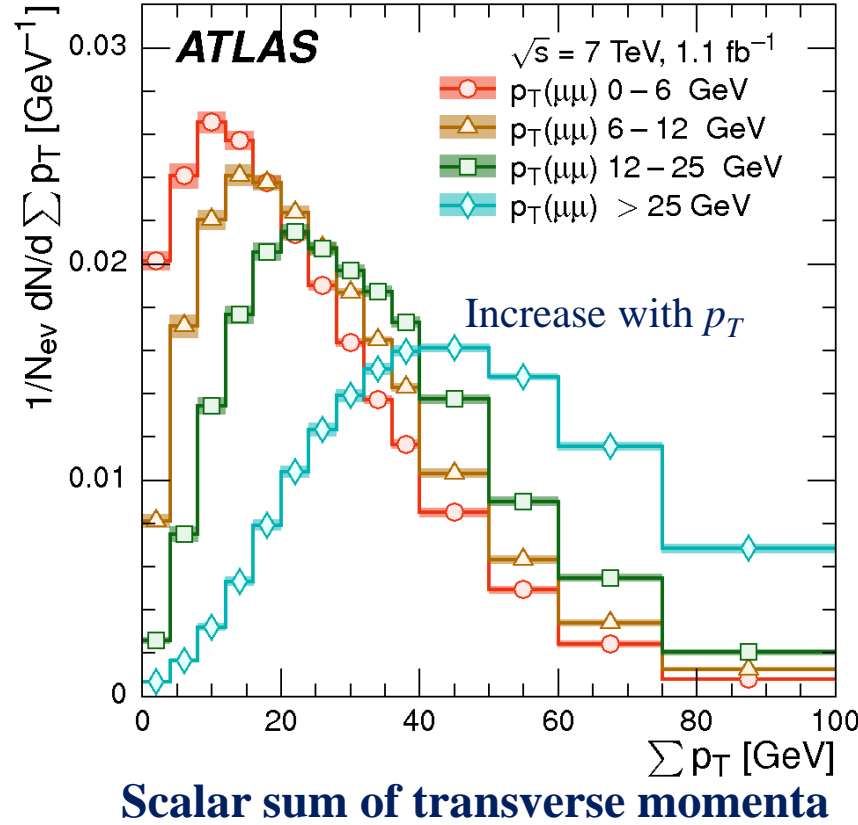
Previous publications:

- ATLAS Collaboration, *Measurement of distributions sensitive to the underlying event in inclusive Z-boson production in pp collisions at $\sqrt{s} = 7$ TeV with the ATLAS detector*; *Eur. Phys. J. C74 (2014) 3195*
- ATLAS Collaboration, *Measurement of the underlying event in jet events from $\sqrt{s}=7$ TeV proton–proton collisions with the ATLAS detector*; *Eur. Phys. J. C74 (2014) 2965*

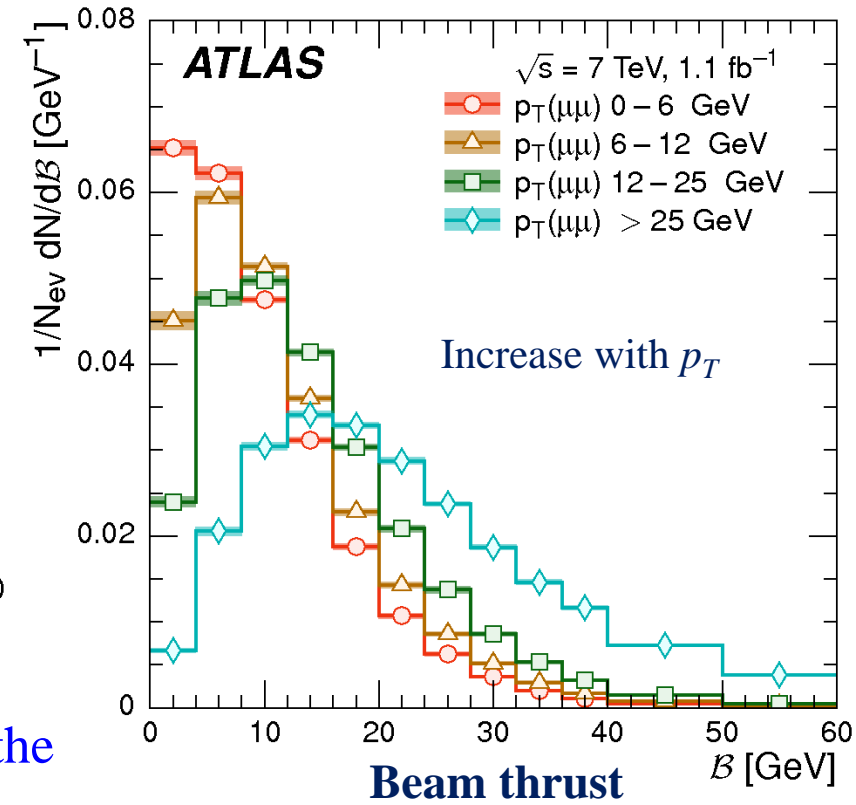


Event-shape distributions for $Z \rightarrow \mu^+ \mu^-$

Recoiling Jet emerging for higher $p_T(\mu^+ \mu^-)$



Similar distributions for $Z \rightarrow e^+ e^-$



4 phase-space regions:

$p_T(\ell) < 6 \text{ GeV}$

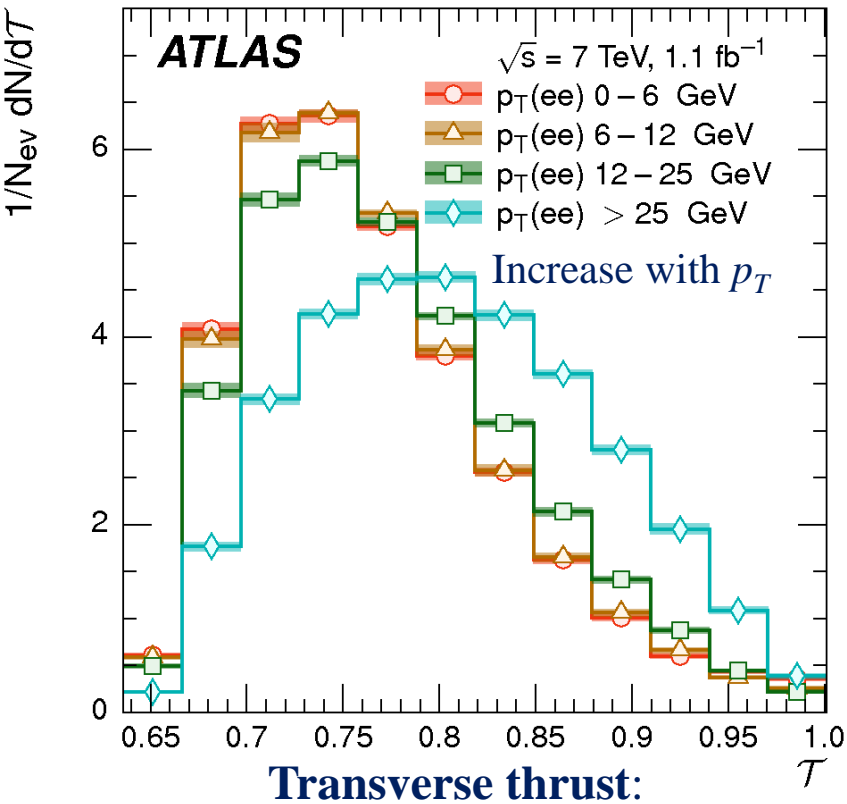
$p_T(\ell) = 6 - 12 \text{ GeV}$

$p_T(\ell) = 12 - 25 \text{ GeV}$

$p_T(\ell) > 25 \text{ GeV}$

The unfolded electron (muon) channel results for the observables in the various $p_T(\ell^+ \ell^-)$ ranges, with the total uncertainty presented as the quadratic sum of the statistical and total systematic uncertainties.

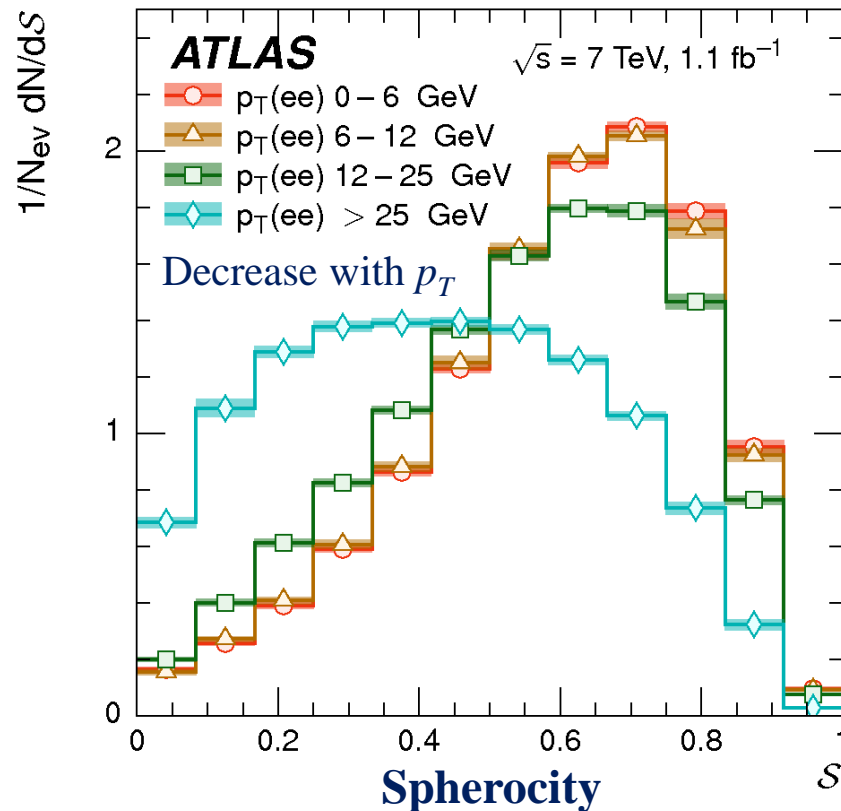
$$B = \sum p_T e^{-|\eta|}$$



$$T = \max_{\vec{n}_T} \frac{\sum |\vec{p}_T \cdot \vec{n}_T|}{\sum p_T}$$

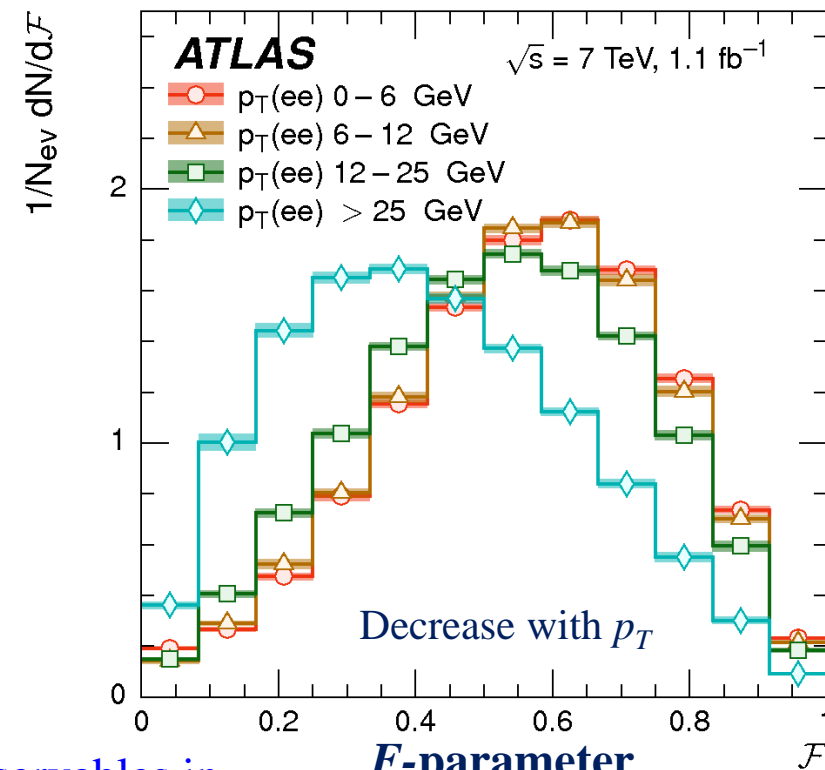
Event-shape distributions in $Z \rightarrow e^+e^-$

$$S = \frac{\pi^2}{4} \min_{\vec{n}=(n_x, n_y, 0)^T} \left(\frac{\sum |\vec{p}_T \times \vec{n}|}{\sum p_T} \right)^2$$



Recoiling Jet emerging for higher $p_T(e^+e^-)$

Similar distributions for $Z \rightarrow \mu^+\mu^-$



$$F = \frac{\lambda_1}{\lambda_2}$$

The unfolded electron (muon) channel results for the observables in the various $p_T(l^+l^-)$ ranges, with the total uncertainty presented as the quadratic sum of the statistical and total systematic uncertainties.

Event-shape observable *Spherocity* in $Z \rightarrow \mu^+\mu^-$ for p_T regions

arXiv: 1602.08980

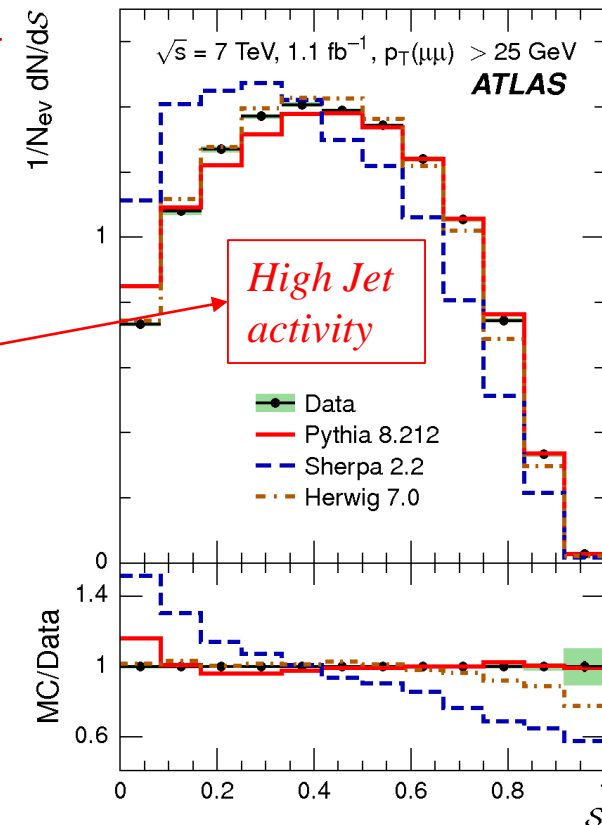
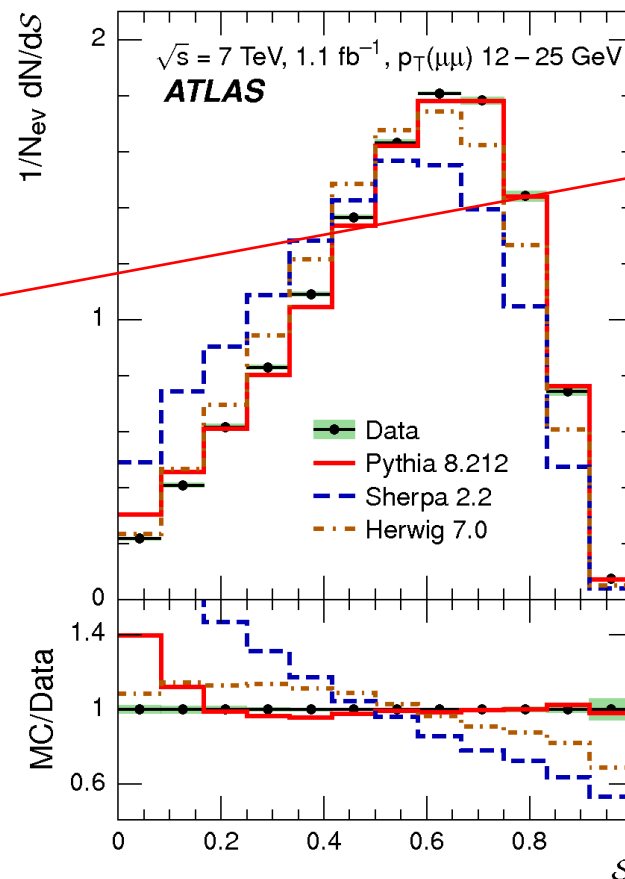
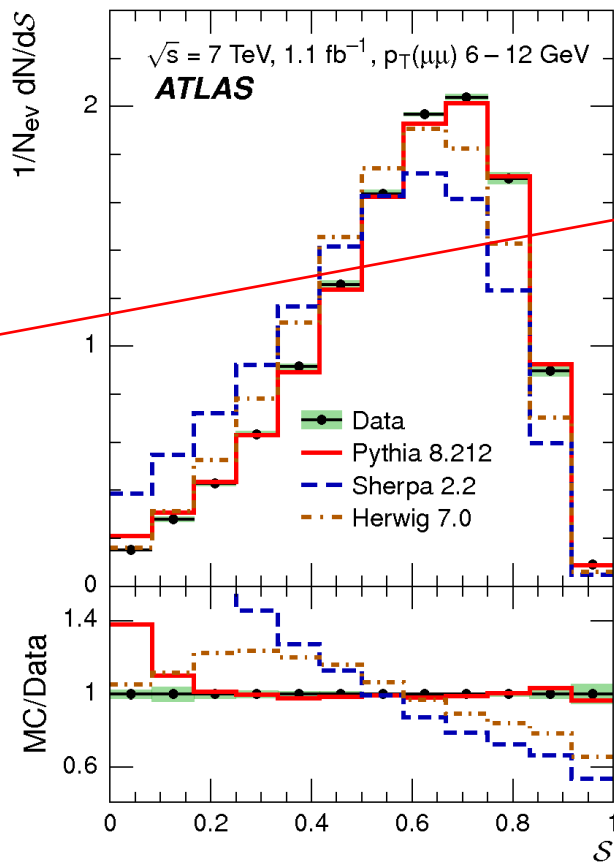
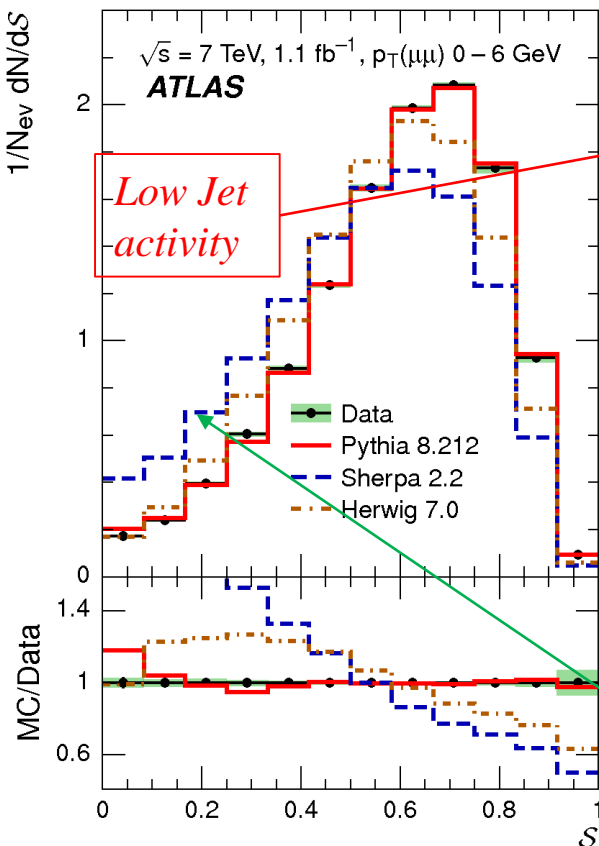
$$\frac{1}{N_{ev}} \frac{dN}{dS} \text{ vs. } S$$

$$S = \frac{\pi^2}{4} \min_{\vec{n}=(n_x, n_y, 0)^T} \left(\frac{\sum |\vec{p}_T \times \vec{n}|}{\sum p_T} \right)^2$$

Event-shape distributions for $Z \rightarrow \mu^+\mu^-$

Similar distributions for $Z \rightarrow e^+e^-$

Underline Event sensitively region



Best agreement for Pythia, Herwig and Sherpa at large p_T

Larger deviations with Sherpa at low p_T

Spherocity S for $Z \rightarrow \mu^+\mu^-$ for the four $p_T(\mu^+\mu^-)$ ranges: 0-6, 6-12, 12-25, ≥ 25 GeV compared to the predictions Pythia8, Sherpa, and Herwig7.

Event-shape observable F -parameter in $Z \rightarrow e^+e^-$ for p_T regions

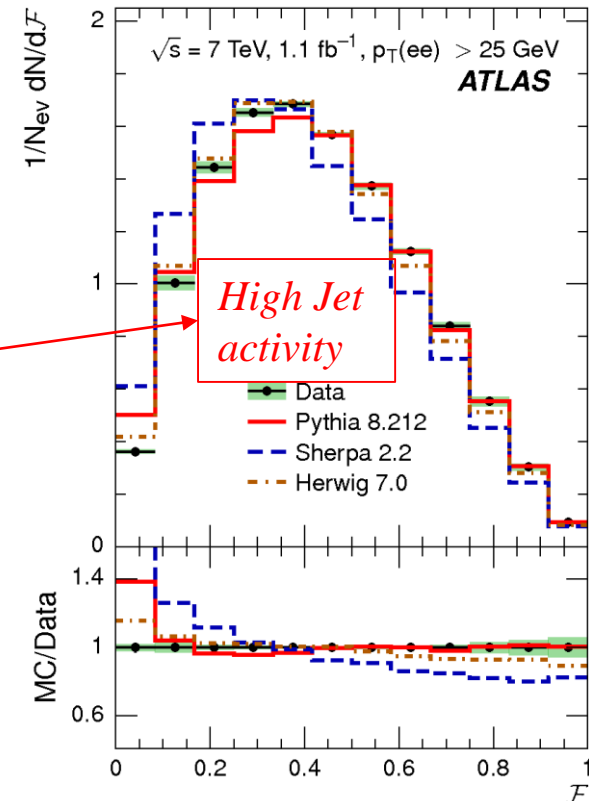
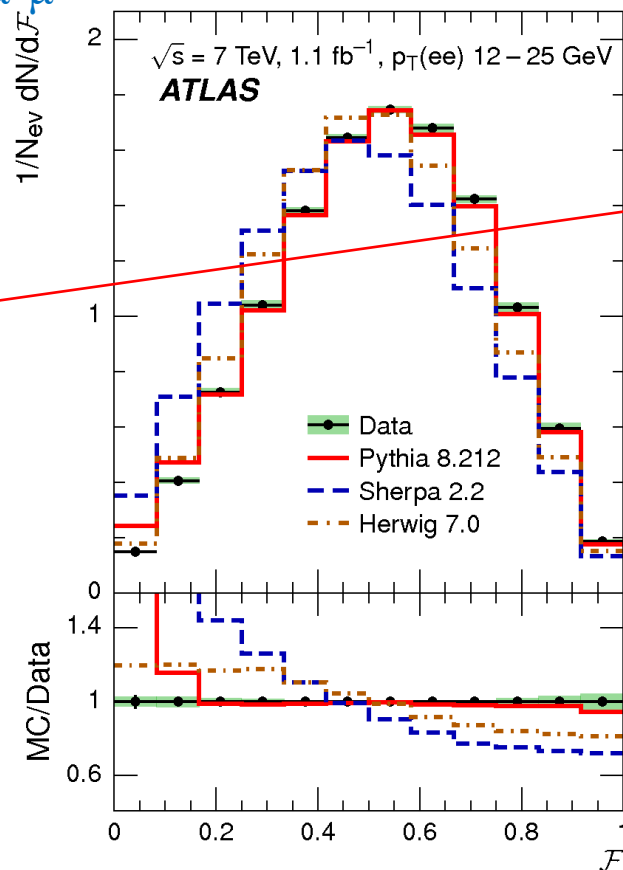
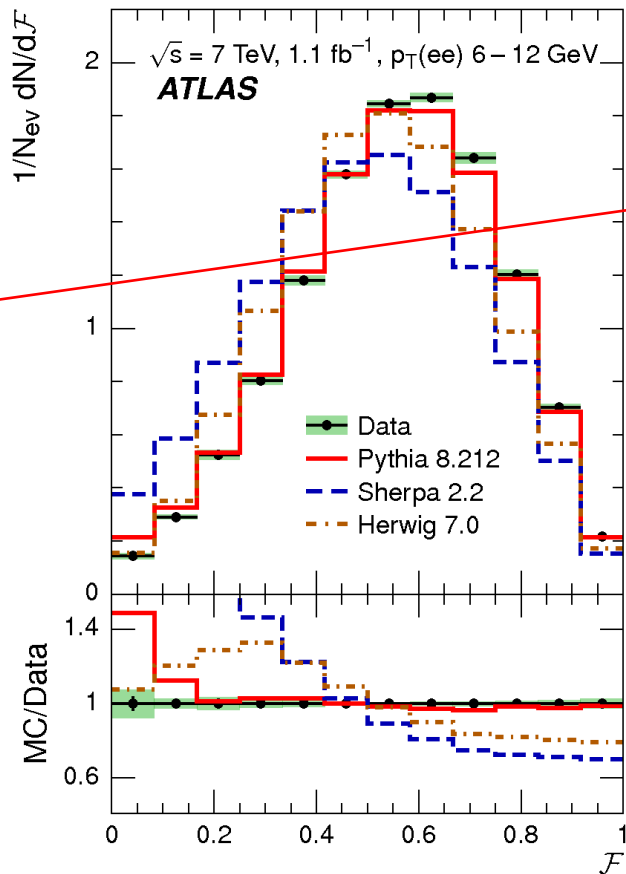
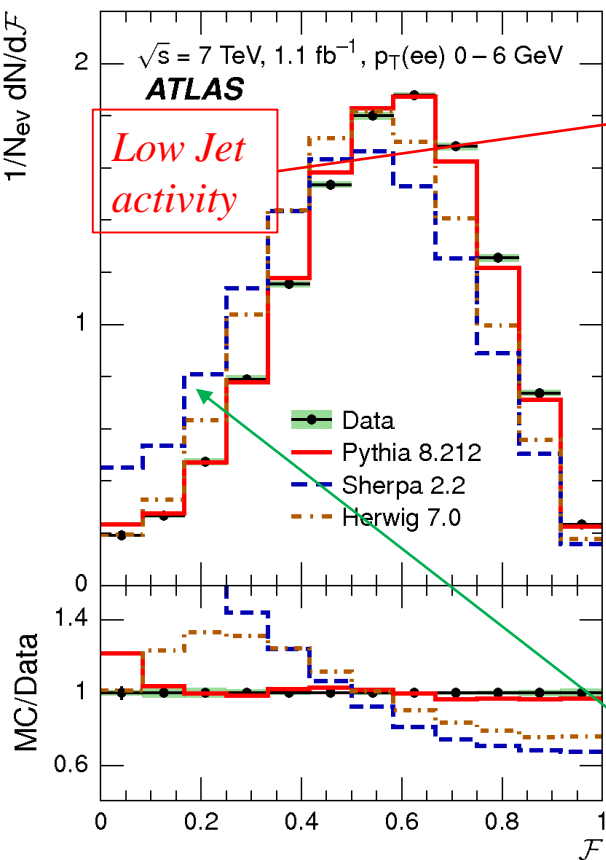
arXiv: 1602.08980

$$\frac{1}{N_{ev}} \frac{dN}{dF} \text{ vs. } F \quad F = \frac{\lambda_1}{\lambda_2}$$

Event-shape distributions in $Z \rightarrow e^+e^-$

Similar distributions for $Z \rightarrow \mu^+\mu^-$

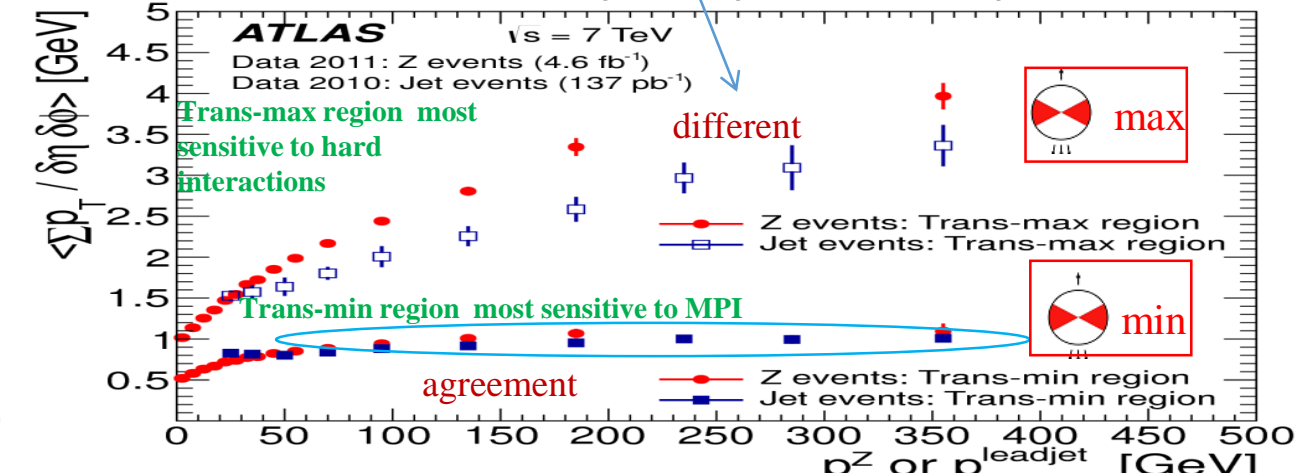
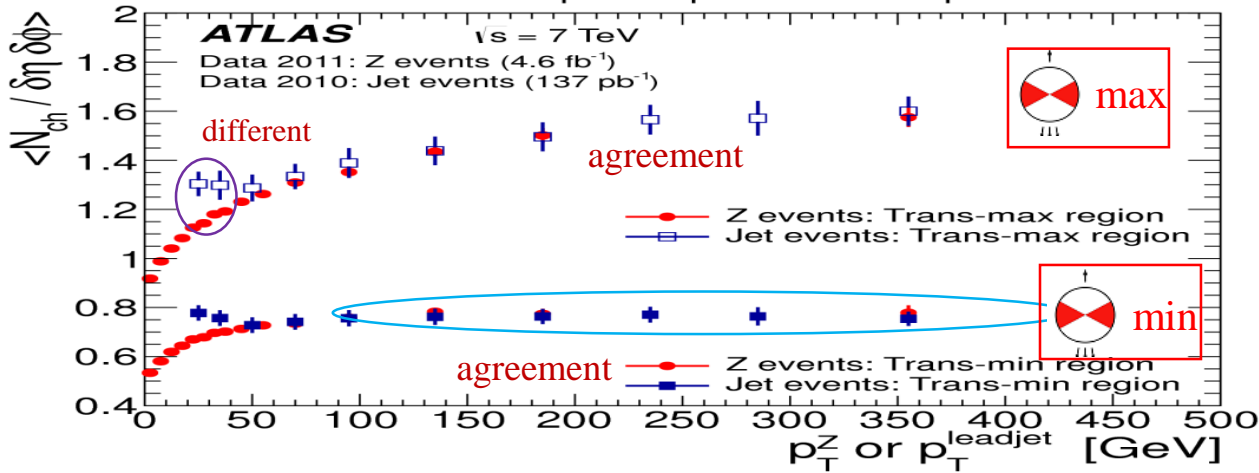
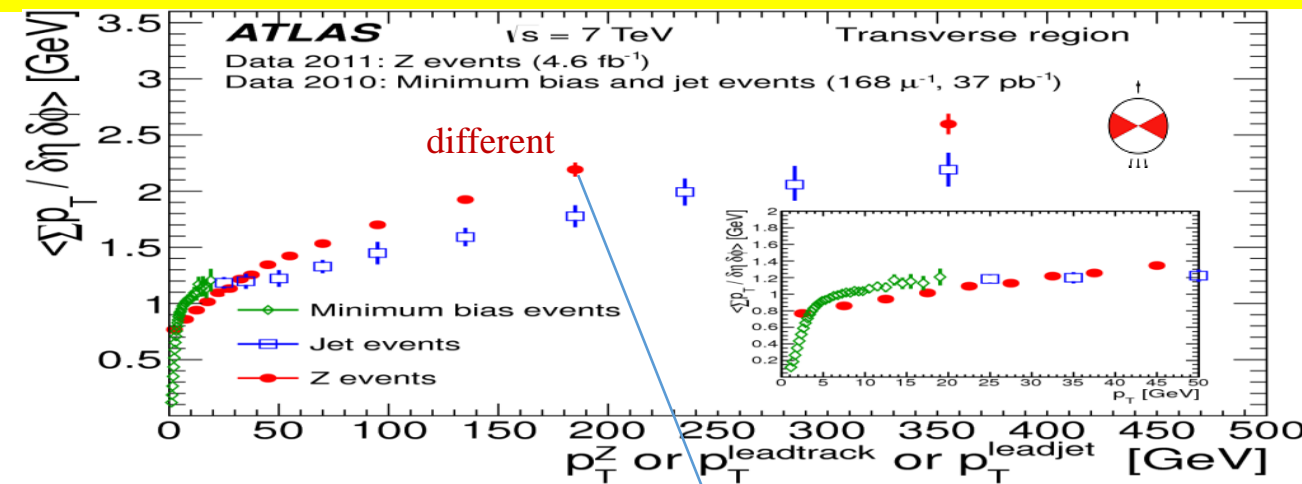
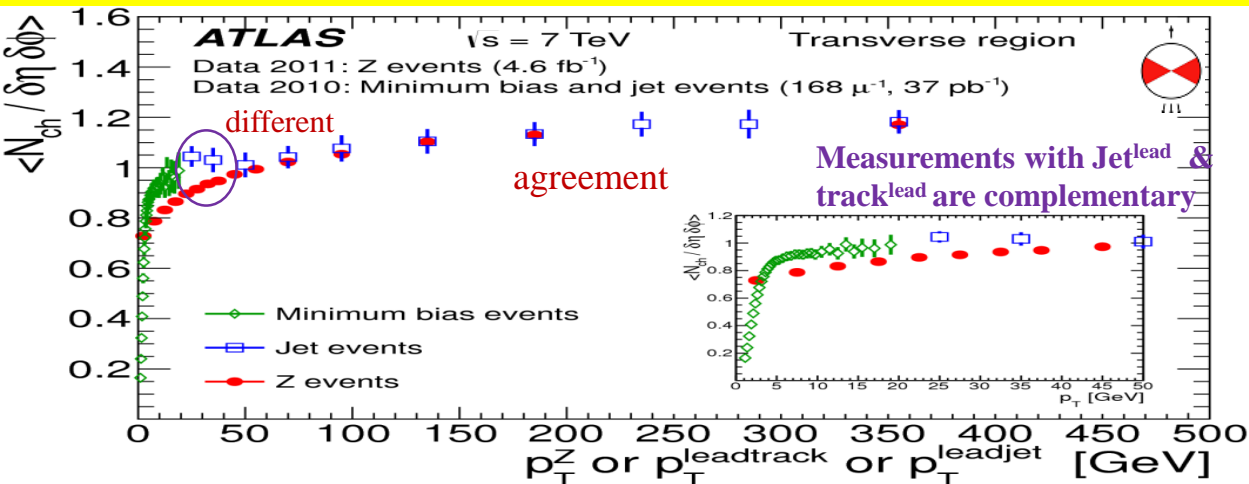
Underline Event sensitively region



Larger deviations with Sherpa at low p_T

Best agreement for Pythia, Herwig and Sherpa at large p_T

F -parameter for $Z \rightarrow \mu^+\mu^-$ for the four $p_T(\mu^+\mu^-)$ ranges: 0-6, 6-12, 12-25, ≥ 25 GeV compared to the predictions Pythia8, Sherpa, and Herwig7. 26

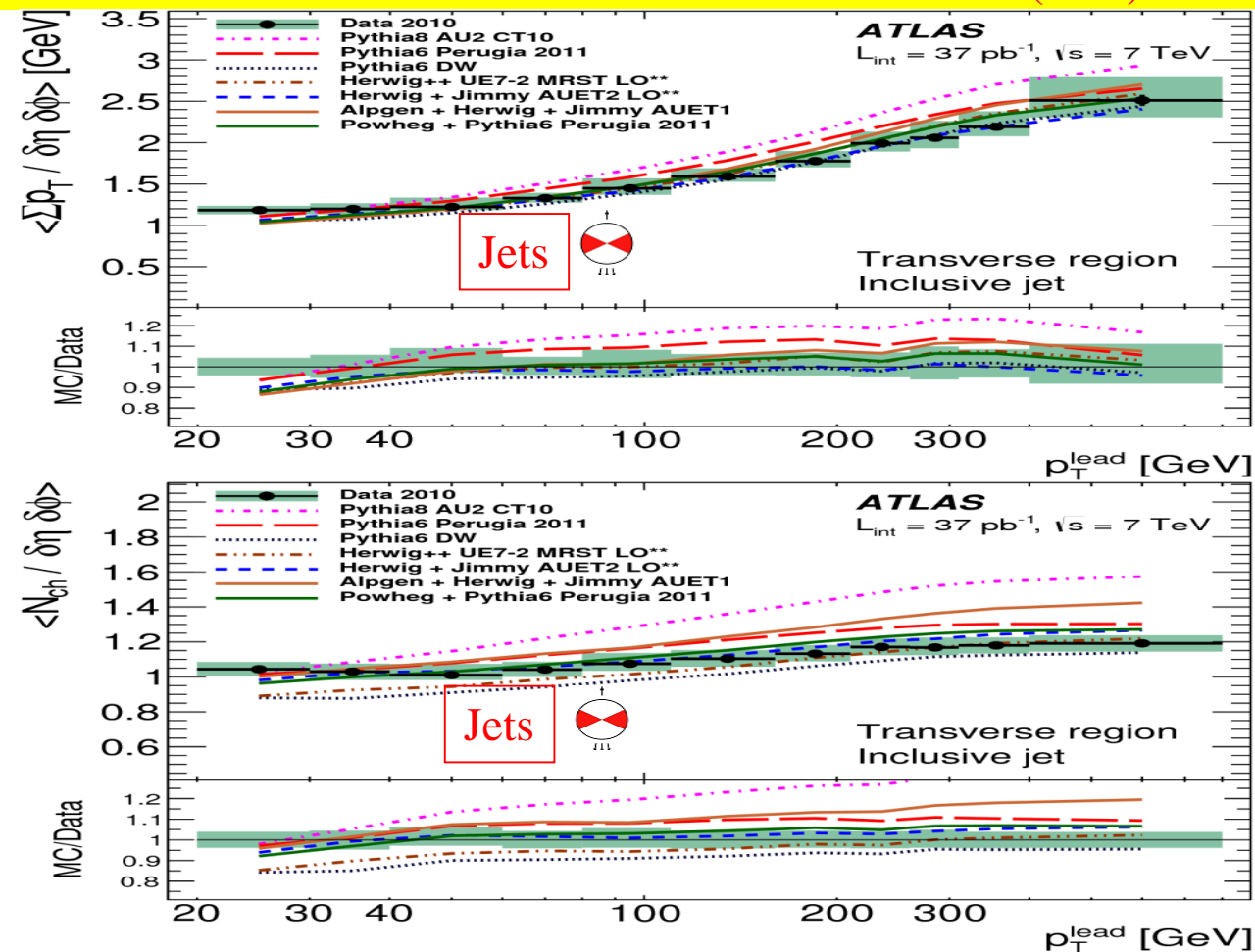
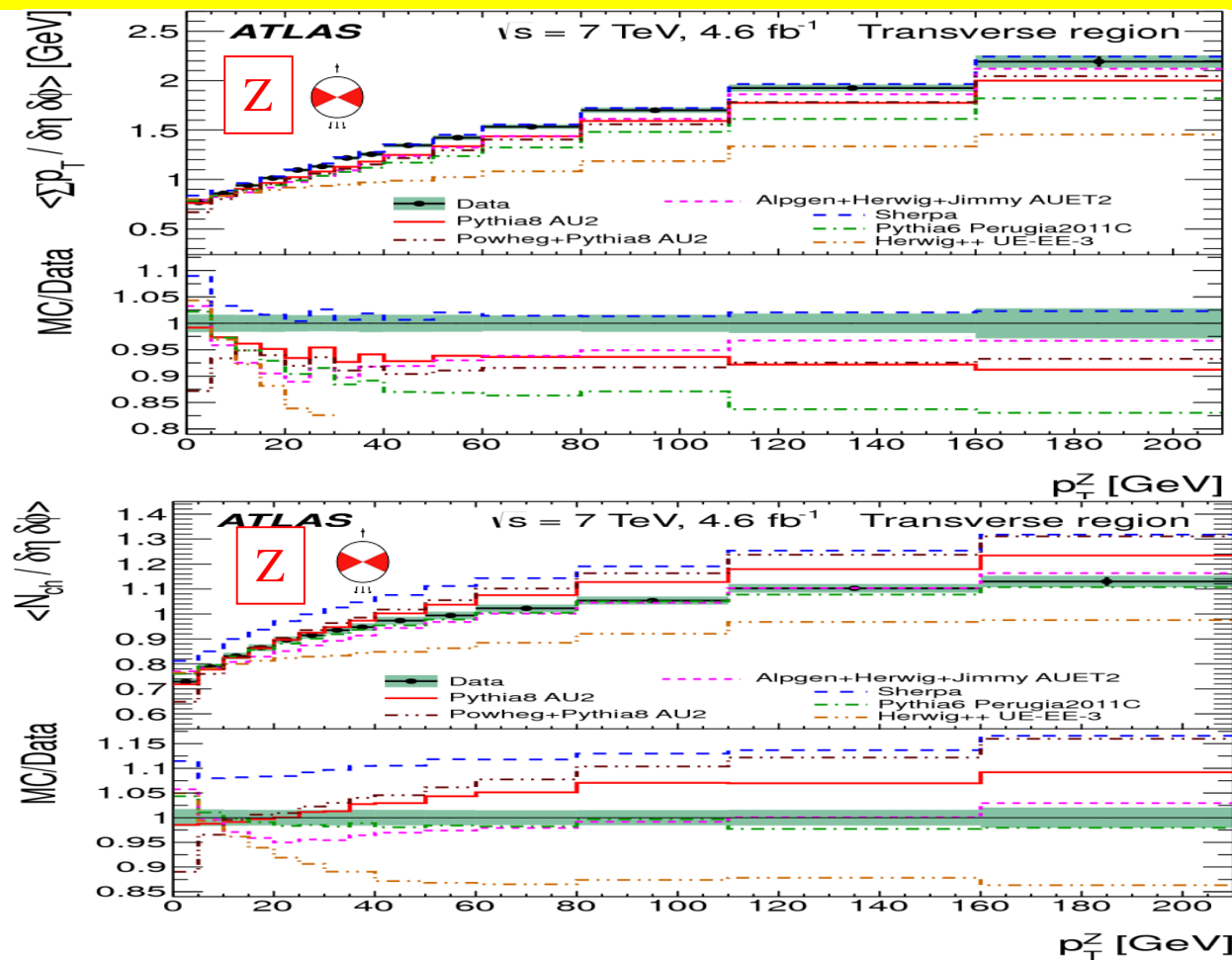


Charged particle multiplicity average values (left) and scalar p_T sum density average values (right) compared between leading charged particle (MB), leading jet and Z boson events, respectively as functions of leading track p_T , leading jet p_T and Z boson p_T .

- ▶ Data are compatible between the different definitions
- ▶ Transition between leading track and jet
- ▶ In the track density distribution, Z-bosons and jets agree well at high p_T

Underlying event *Z* and *Jets* at 7 TeV

EPJC 74 (2014) 3195
EPJC 74 (2014) 2965



Comparison of detector level data and MC predictions for average scalar p_T sum density of tracks (top row) and average track multiplicity density values (bottom row) as a function of *Z* (left column) and leading jet (right column) transverse momentum.

- For *Jets*: Not perfect agreement between data and simulation **Herwig** better than **Pythia6**
- For *Z*: Good description given by **Sherpa**, followed by **Pythia 8**, **ALPGEN** and **POWHEG**